AD-A041 762 CALIFORNIA STATE UNIV LONG BEACH DEPT OF MECHANICAL --ETC F/G 13/10
A GENERAL METHOD FOR CALCULATING THREE-DIMENSIONAL LAMINAR AND --ETC(U)
APR 77 T CEBECI, K CHANG N00014-76-C-0901
UNCLASSIFIED CSULB-TR-77-1 NL

1 OF 1
ADA041762

END

DATE
FILMED
8 - 77

A GENERAL METHOD FOR CALCULATING THREE-DIMENSIONAL LAMINAR AND TURBULENT BOUNDARY LAYERS ON SHIP HULLS

I. COORDINATE SYSTEM, NUMERICAL METHOD AND PRELIMINARY RESULTS

TUNCER CEBECI and K. C. CHANG

DEPARTMENT OF MECHANICAL ENGINEERING
CALIFORNIA STATE UNIVERSITY AT LONG BEACH
LONG BEACH, CALIFORNIA
90840

CONTRACT NO. N00014-76-C-0901

APRIL 1977

PREPARED FOR THE

OFFICE OF NAVAL RESEARCH • 800 N. QUINCY ST. • ARLINGTON•VA•22217

A GENERAL METHOD FOR CALCULATING THREE-DIMENSIONAL LAMINAR AND TURBULENT BOUNDARY LAYERS ON SHIP HULLS

I. COORDINATE SYSTEM, NUMERICAL METHOD AND PRELIMINARY RESULTS

TUNCER CEBECI and K. C. CHANG

DEPARTMENT OF MECHANICAL ENGINEERING
CALIFORNIA STATE UNIVERSITY AT LONG BEACH
LONG BEACH, CALIFORNIA
90840

CONTRACT NO. N00014-76-C-0901

APRIL 1977

PREPARED FOR THE

OFFICE OF NAVAL RESEARCH • 800 N. QUINCY ST. • ARLINGTON•VA•22217

UNCLASSIFIED

SECURITY CLASSIFICATION OF THIS PAGE (When Data Entered)

REPORT DOCUMENTATION PAGE	READ INSTRUCTIONS BEFORE COMPLETING FORM
1. REPORT NUMBER: CSULB-TR-77-1	2. GOVT ACCESSION NO.
3. RECIPIENT'S CATALOG NUMBER	
4. TITLE (and Subtitle): A General Method for Calculating Three-Dimensional Laminar and Turbulent Boundary Layers on Ship Hulls. I. Coordinate System, Numerical Method and Preliminary Results.	5. TYPE OF REPORT & PERIOD COVERED: Final rept. Jun 76 - Apr 1977
	6. PERFORMING ORG. REPORT NUMBER
7. AUTHOR(s): Tuncer Cebeci K. C. Chang	8. CONTRACT OR GRANT NUMBER(s): N00014-76-C-0901
9. PERFORMING ORGANIZATION NAME AND ADDRESS: Mechanical Engineering Department, California State University at Long Beach, Long Beach, California 90840	10. PROGRAM ELEMENT, PROJECT, TASK AREA & WORK UNIT NUMBERS: NR 061-246
11. CONTROLLING OFFICE NAME AND ADDRESS: Office of Naval Research, 800 N. Quincy Street, Arlington, Va. 22217	12. REPORT DATE: Apr 1977
	13. NUMBER OF PAGES: 43
14. MONITORING AGENCY NAME & ADDRESS (if different from Controlling Office)	15. SECURITY CLASS. (of this report): Unclassified
	15a. DECLASSIFICATION/DOWNGRADING SCHEDULE

16. DISTRIBUTION STATEMENT (of this Report)

Approved for public release; distribution unlimited

17. DISTRIBUTION STATEMENT (of the abstract entered in Block 20, if different from Report)

18. SUPPLEMENTARY NOTES

19. KEY WORDS (Continue on reverse side if necessary and identify by block number)

three-dimensional boundary layers
ship hull
metric coefficients & geodesic curvatures
eddy viscosity

20. ABSTRACT (Continue on reverse side if necessary and identify by block number)

This report describes the progress made during the past year towards the development of a general method for computing three-dimensional incompressible laminar and turbulent boundary layers on ship hulls. The method employs an implicit two-point finite-difference method developed by Keller and Cebeci and an algebraic eddy-viscosity formulation developed by Cebeci. During the past year the efforts concentrated on the choice of an appropriate coordinate system; the calculation of the geometric parameters of this coordinate system;

DD FORM 1 JAN 73 1473 EDITION OF 1 NOV 65 IS OBSOLETE
S/N 0102-014-6601

Unclassified
SECURITY CLASSIFICATION OF THIS PAGE (When Data Entered)

409 265

the numerical solution of the governing equation for the orthogonal curvilinear system; and obtaining preliminary results for simple ship forms. Further studies are in progress and will be reported in a forthcoming report.

TABLE OF CONTENTS

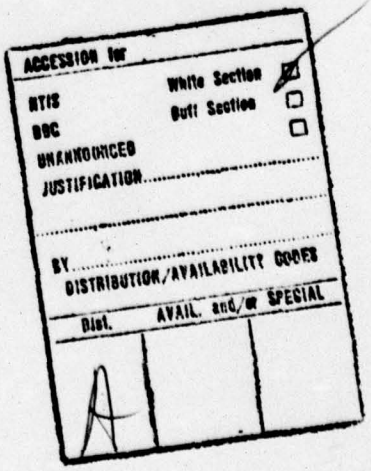

PRINCIPAL NOTATION

A	Van Driest damping parameter, see (2.20b)
cf_s	local skin friction coefficient in streamwise direction
f	transformed vector potential for ψ
g	transformed vector potential for Φ
h_1, h_2	metric coefficients
h_j	net spacing in η-direction
h_z	metric coefficient, see (2.15)
H	boundary-layer shape factor, δ^*/θ_{11}
k_n	net spacing in x-direction
K_1, K_2	geodesic curvatures, see (2.5)
L	mixing length, see (2.20a)
p	static pressure
q_e	magnitude of velocity vector at the boundary-layer edge
q_s, q_n	velocity components in boundary-layer parallel and normal, respectively, to external streamline
R_s	Reynolds number, $u_e s_1/\nu$
R_θ	Reynolds number, $q_e\theta_{11}/\nu$
s	arc length along coordinate line
u,v,w	velocity components in the x_1, y, x_2 directions
u_τ	friction velocity, see (2.20c)
u_∞	freestream velocity
u_{ref}	reference velocity
x_1	curvilinear surface coordinate
x_2	curvilinear surface coordinate orthogonal to the x-coordinate
y, x_3	distance normal to the body surface

x,y,z	Cartesian coordinates
$-\rho\overline{u'v'}$, $-\rho\overline{u'w'}$	Reynolds stresses
δ	boundary-layer thickness
δ^*	displacement thickness, $\int_0^\infty (1 - q_s/q_e)dy$
ε_m	eddy viscosity
ε_m^+	dimensionless eddy viscosity, ε_m/ν
η	similarity variable for y, see (2.22)
θ_{11}	momentum thickness, $\int_0^\infty q_s/q_e(1 - q_s/q_e)dy$
μ	dynamic viscosity
ν	kinematic viscosity
ρ	density
τ	shear stress
ϕ,ψ	two-component vector potential, see (2.23a)

Subscripts

e	boundary-layer edge
s	streamwise direction
w	wall

Primes denote differentiation with respect to η

1.0 INTRODUCTION

The work reported here describes the progress made during the past year towards the development of a general method for computing three-dimensional incompressible laminar and turbulent boundary layers on ship hulls. The method employs an implicit two-point finite-difference method developed by Keller and Cebeci[1] and an algebraic eddy-viscosity formulation developed by Cebeci[2]. During the past year our efforts concentrated on the choice of an appropriate coordinate system; the calculation of the geometric parameters of this coordinate system; the numerical solution of the governing equations for the orthogonal curvilinear system; and obtaining preliminary results for simple ship forms.

In Section 2 we discuss the basic equations and the coordinate system. The governing equations which,in Section 2.1, are written for three-dimensional incompressible laminar and turbulent flows in an orthogonal curvilinear coordinate system require initial conditions on two intersecting lines. For this reason, in Section 2.2, we discuss the formulation of the governing equations to generate these initial conditions.

In principle, the calculation of boundary-layer development on ship hulls can be achieved in a number of coordinate systems applicable to arbitrary three-dimensional bodies. The presence of the free surface suggests the use of a streamline coordinate system because the flow boundaries and the coordinate lines in that system coincide. In our study, however, we abandon this system in favor of a body-oriented one (see Section 2.2) suggested by Miloh and Patel[3], which avoids the complexity of calculating the streamline coordinates for each Froude number. Consequently, the coordinate system and its geometrical parameters such as the metric coefficients and the geodesic curvatures are computed once and for all for a specified ship hull. If the ship hull is described in analytic form, then these geometric parameters can be computed exactly. For arbitrary ship hulls, they must be computed numerically. We discuss this aspect of the problem in Appendix A.

For turbulent flows, the governing equations require closure assumptions for the Reynolds stresses. Here we use the eddy-viscosity concept and model the Reynolds shear stress terms by an algebraic eddy-viscosity formulation developed by Cebeci[2]. This phase of the problem is discussed in Section 2.4.

When physical coordinates are used, solutions of the governing boundary-layer equations are sensitive to the net spacings in the streamwise direction (x) and the crosswise direction (z), and require a large number of x- and z-stations. To remove this sensitivity and to generate the initial conditions, we express the governing equations in transformed coordinates. For this reason, in Section 2.5, we discuss a convenient transformation and express the boundary-layer equations in terms of transformed variables.

In Section 3 we describe the numerical method used to solve the basic equations for both laminar and turbulent flows, and in Section 4 we present preliminary results for a double-elliptic ship model. These sections are followed by a discussion section (Section 5) where we outline the work planned for the next phase of the studies. Finally, in Appendix B we present a user's manual for the computer program.

2.0 BASIC EQUATIONS AND THE COORDINATE SYSTEM

2.1 Boundary-Layer Equations

The governing boundary-layer equations for three-dimensional incompressible laminar and turbulent flows in a curvilinear orthogonal coordinate system are given by:

Continuity Equation

$$\frac{\partial}{\partial x_1}(h_2 u) + \frac{\partial}{\partial x_2}(h_1 w) + \frac{\partial}{\partial x_3}(h_1 h_2 v) = 0 \tag{2.1}$$

x_1-Momentum Equation

$$\frac{u}{h_1}\frac{\partial u}{\partial x_1} + \frac{w}{h_2}\frac{\partial u}{\partial x_2} + v\frac{\partial u}{\partial x_3} + K_2 w^2 - K_1 uw = -\frac{1}{h_1}\frac{\partial}{\partial x_1}\left(\frac{p}{\rho}\right) + \frac{\partial}{\partial x_3}\left(\nu\frac{\partial u}{\partial x_3} - \overline{u'v'}\right) \tag{2.2}$$

x_2-Momentum Equation

$$\frac{u}{h_1}\frac{\partial w}{\partial x_1} + \frac{w}{h_2}\frac{\partial w}{\partial x_2} + v\frac{\partial w}{\partial x_3} + K_1 u^2 - K_2 uw = -\frac{1}{h_2}\frac{\partial}{\partial x_2}\left(\frac{p}{\rho}\right) + \frac{\partial}{\partial x_3}\left(\nu\frac{\partial w}{\partial x_3} - \overline{u'w'}\right) \tag{2.3}$$

Here h_1 and h_2 are the metric coefficients and they are, in general, functions of x_1 and x_2, that is,

$$h_1 = h_1(x_1, x_2) \qquad h_2 = h_2(x_1, x_2) \tag{2.4}$$

The parameters K_1 and K_2 are known as the geodesic curvatures of the curves x_2 = constant and x_1 = constant, respectively. They are defined as

$$K_1 = -\frac{1}{h_1 h_2}\frac{\partial h_1}{\partial x_2} \qquad K_2 = -\frac{1}{h_1 h_2}\frac{\partial h_2}{\partial x_1} \tag{2.5}$$

At the edge of the boundary layer, (2.2) and (2.3) reduce to

$$\frac{u_e}{h_1}\frac{\partial u_e}{\partial x_1} + \frac{w_e}{h_2}\frac{\partial u_e}{\partial x_2} + K_2 w_e^2 - K_1 u_e w_e = -\frac{1}{h_1}\frac{\partial}{\partial x_1}\left(\frac{p}{\rho}\right) \tag{2.6a}$$

$$\frac{u_e}{h_1}\frac{\partial w_e}{\partial x_1} + \frac{w_e}{h_2}\frac{\partial w_e}{\partial x_2} + K_1 u_e^2 - K_2 u_e w_e = -\frac{1}{h_2}\frac{\partial}{\partial x_2}\left(\frac{p}{\rho}\right) \tag{2.6b}$$

The boundary conditions for equations (2.1) to (2.3) are:

$$x_3 = 0 \qquad u, v, w = 0 \tag{2.7a}$$

$$x_3 = \delta \qquad u = u_e(x_1, x_2) \qquad w = w_e(x_1, x_2) \tag{2.7b}$$

2.2 Initial Conditions

The solution of the system given by (2.1) to (2.3) subject to (2.7) requires closure assumptions for the Reynolds stresses, $-\rho\overline{u'v'}$ and $-\rho\overline{v'w'}$. They also require initial conditions on two intersecting planes. In general, the construction of these initial conditions for three-dimensional flows on arbitrary bodies such as ship hulls is rather difficult due to a variety of bow shapes which may be quite complicated. For this reason, it is necessary to make some assumptions for them in order to start the calculations.

In our study we choose the inviscid dividing streamline on which $\partial p/\partial x_2 = 0$ to be one of the initial data line (see Figure 1). In the case of a rectilinear

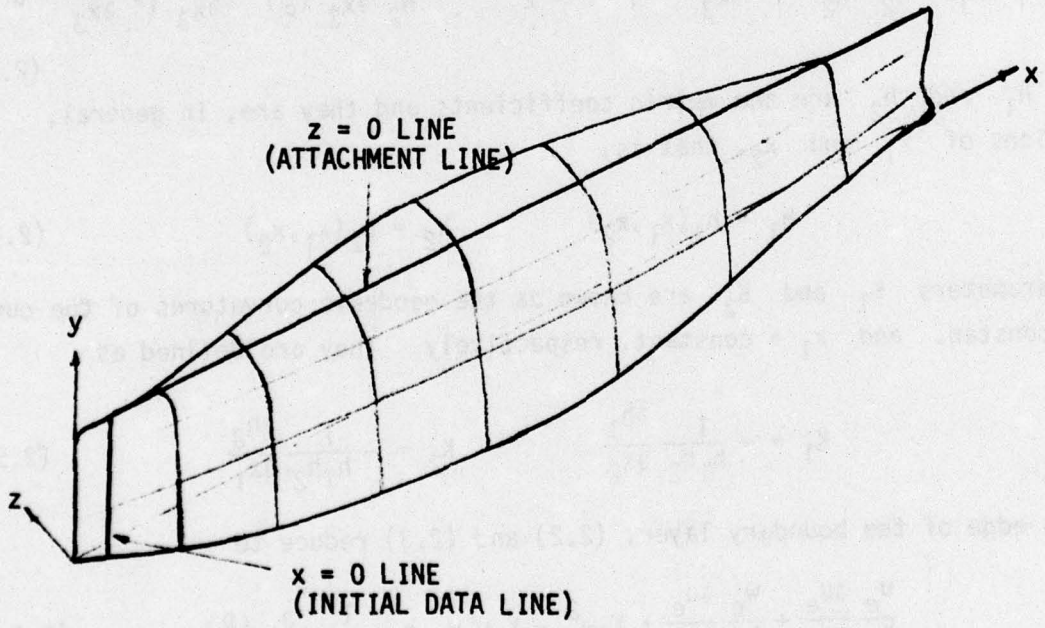

Figure 1. A sketch of the initial data lines

motion of a ship, this streamline runs along the plane of symmetry. We also select this line as the $x_2 = 0$ line for the coordinate system. Because of the symmetry conditions w and K_1 are zero on this line causing (2.3) to become singular. However, differentiation with respect to x_2 yields a nonsingular equation. After performing the necessary differentiation for the x_2-momentum equation and taking advantage of appropriate symmetry conditions in (2.3) and in the other equations, we can write the so-called streamwise attachment-line equations as:

Continuity Equation:

$$\frac{\partial}{\partial x_1}(h_2 u) + h_1 h_2 w_z + \frac{\partial}{\partial x_3}(h_1 h_2 v) = 0 \tag{2.8}$$

x_1-Momentum Equation:

$$\frac{u}{h_1}\frac{\partial u}{\partial x_1} + v\frac{\partial u}{\partial x_3} = \frac{u_e}{h_1}\frac{\partial u_e}{\partial x_1} + \frac{\partial}{\partial x_3}\left(\nu\frac{\partial u}{\partial x_3} - \overline{u'v'}\right) \tag{2.9}$$

x_2-Momentum Equation

$$\frac{u}{h_1}\frac{\partial w_z}{\partial x_1} + w_z^2 + v\frac{\partial w_z}{\partial x_3} - K_2 u w_z + \frac{\partial K_1}{h_2 \partial x_2}u^2 = \frac{u_e}{h_1}\frac{\partial w_{ze}}{\partial x_1} + w_{ze}^2 - K_2 u_e w_{ze} + \frac{\partial K_1}{h_2 \partial x_2}u_e^2 + \frac{\partial}{\partial x_3}\left[\nu\frac{\partial w_z}{\partial x_3} - (\overline{v'w'})_z\right] \tag{2.10}$$

where $w_z = 1/h_2\ \partial w/\partial x_2$ and $(\overline{v'w'})_z = 1/h_2\ \partial/\partial x_2\ (\overline{v'w'})$. These equations are subject to the following boundary conditions:

$$x_3 = 0 \qquad u = v = w_z = 0 \tag{2.11a}$$

$$x_3 = \delta \qquad u = u_e,\ w_z = w_{ze} \tag{2.11b}$$

The other initial data line should be selected near the bow of the ship along the line perpendicular to the x_2 = const. coordinate. However, because of the variety of bow shapes possible, some of which may be quite complicated, it is necessary to make further simplifying approximations to the flow on the line. In our study we assume the flow along the initial line to be two-dimensional without pressure gradient, and solve the governing two-dimensional equations for a flat plate.

2.3 Coordinate System

Since, in general, a ship form is a rather complex nondevelopable surface, a Cartesian coordinate system is not suitable for boundary-layer calculations. The streamline coordinate system is a very attractive one. The determination of the streamlines, the orthogonal lines and the associated geometrical parameters require considerable work. In addition, they are dependent on the Froude number and the Reynolds number if the displacement effect is taken into account. Consequently, this coordinate system, in addition to being hard to compute, becomes also uneconomical to use when the effects of the Froude number and the Reynolds number are to be systematically investigated.

In selecting a coordinate system for the boundary-layer calculations, it is desirable to choose one such that it is calculated only once. Although a general nonorthogonal coordinate system has been developed with success by Cebeci, Kaups and Ramsey[4], the numerical work for evaluating the geometrical parameters is very involved. For this reason, in the present study, we have decided to abandon this coordinate system in favor of the one suggested by Miloh and Patel[3]. This coordinate system depends only on the geometry of the body and is calculated once and for all. Therefore, the effects of the draft, the trim, the Froude number, and the Reynolds number on ship boundary-layer development can be systematically studied. In this coordinate system, one of the coordinates is taken as the lines of x_1 = constant. The other coordinate $x_2(x,z)$ constant, which is orthogonal to x_1 = constant lines everywhere on the ship hull, can be shown to be the solution of the differential equation

$$\frac{dz}{dx} = -\frac{f_x f_z}{1 + f_z^2} \tag{2.12}$$

Here $y = f(x,z)$ defines the ship hull, and (x,y,z) denote the Cartesian coordinates. The geometrical parameters are calculated from the following formulas

$$h_1 = \left(1 + \frac{f_x^2}{1 + f_z^2}\right)^{1/2} \tag{2.13a}$$

$$h_2 = \frac{(1 + f_z^2)^{1/2}}{\partial x_2/\partial z} \tag{2.13b}$$

$$K_1 = -\frac{f_x[f_{xz}(1 + f_z^2) - f_x f_z f_{zz}]}{(1 + f_z^2)^{3/2}\,(1 + f_x^2 + f_z^2)} \tag{2.13c}$$

$$K_2 = \frac{f_x f_{zz}}{(1 + f_z^2)^{3/2}\,(1 + f_z^2 + f_x^2)^{1/2}} \tag{2.13d}$$

It may be noted that K_1 and K_2 can also be obtained from (2.5). This provides a check on the expressions given above.

In the boundary-layer equations, h_2 always occurs in the combination $1/h_2\ \partial/\partial x_2$. Since we have chosen x and x_2 as independent variables, we have

$$\frac{1}{h_2}\frac{\partial}{\partial x_2} = \frac{1}{h_2}\frac{\partial z}{\partial x_2}\frac{\partial}{\partial x_z} = \frac{1}{h_z}\frac{\partial}{\partial x_z} \tag{2.14}$$

where

$$h_z = h_2 \frac{\partial x_2}{\partial z} \tag{2.15}$$

From (2.13b) it follows that

$$h_z = (1 + f_z^2)^{1/2} \tag{2.16}$$

We see that once the curvatures have been found, it is no longer necessary to work with (x, x_2) coordinates; instead we can work with (x,z) coordinates layers on ship hulls and solve the governing equations in that system. The use of this coordinate system offers the major computational advantage that the pressure distribution can be prescribed much more readily in terms of x and z than in terms of x and x_2.

In the boundary-layer calculations, we need the velocity components along the surface coordinates. For the coordinate system adopted, it can be shown that the velocity components in the two systems are related by[5]

$$u_e = \frac{(1 + f_z^2)U + f_x V - f_x f_z W}{[(1 + f_z^2)(1 + f_x^2 + f_z^2)]^{1/2}} \tag{2.17a}$$

$$w_e = \frac{Vf_z + W}{(1 + f_z^2)^{1/2}} \tag{2.17b}$$

Here (U, V, W) are the velocity components in the Cartesian coordinates, and (u_e, w_e) in the adopted coordinates.

2.4 Turbulence Model

For turbulent flows, it is necessary to make closure assumptions for the Reynolds stresses, $-\rho\overline{u'v'}$ and $-\rho\overline{v'w'}$. In our study, we satisfy this requirement by using the eddy-viscosity concept and relate the Reynolds stresses to the mean velocity profiles by

$$-\overline{u'v'} = \varepsilon_m \frac{\partial u}{\partial y} \qquad -\overline{v'w'} = \varepsilon_m \frac{\partial w}{\partial y} \tag{2.18}$$

Here we have let $x_3 = y$. We use the eddy-viscosity formulation of ref. 2 and define ε_m by two separate formulas. In the inner region, ε_m is defined as

$$(\varepsilon_m)_i = L^2\left[\left(\frac{\partial u}{\partial y}\right)^2 + \left(\frac{\partial w}{\partial y}\right)^2\right]^{1/2} \tag{2.19}$$

where

$$L = 0.4\, y\,[1 - \exp(-y/A)] \tag{2.20a}$$

$$A = 26\nu u_\tau^{-1} \tag{2.20b}$$

$$u_\tau = \nu^{1/2}\left[\left(\frac{\partial u}{\partial y}\right)_w^2 + \left(\frac{\partial w}{\partial y}\right)_w^2\right]^{1/4} \tag{2.20c}$$

In the outer region, ε_m is defined by the following formula:

$$(\varepsilon_m)_o = 0.0168 \left| \int_0^\infty \left(\sqrt{u^2 + w^2} - \sqrt{u_e^2 + w_e^2}\right) dy \right| \tag{2.21}$$

The inner and outer regions are established by the continuity of the eddy-viscosity formula.

2.5 Transformation of the Basic Equations

The boundary-layer equations can be solved either in physical coordinates or in transformed coordinates. Each coordinate system has its own advantage. In three-dimensional flows, the computer time and storage required is an important factor. The transformed coordinates are then favored because the coordinates allow larger steps to be taken in the streamwise and spanwise directions.

We define the transformed coordinates by $(x_3 = y)$

$$x_1 = x_1, \quad x_2 = x_2, \quad d\eta = \left(\frac{u_e}{\nu s_1}\right)^{1/2} dy \qquad s_1 = \int_0^{x_1} h_1 dx_1 \tag{2.22}$$

and introduce a two-component vector potential such that

$$uh_2 = \frac{\partial \psi}{\partial y} \qquad\qquad wh_1 = \frac{\partial \phi}{\partial y} \tag{2.23a}$$

$$vh_1h_2 = -\left(\frac{\partial \psi}{\partial x_1} + \frac{\partial \phi}{\partial x_2}\right) \tag{2.23b}$$

where ψ and ϕ are defined as

$$\psi = (\nu u_e s_1)^{1/2} h_2 f(x_1, x_2, \eta) \tag{2.24a}$$

$$\phi = (\nu u_e s_1)^{1/2} u_{ref}/u_e \; h_1 g(x_1, x_2, \eta) \tag{2.24b}$$

and u_{ref} is some reference velocity.

Using these transformations and the relations given by (2.6) and (2.12), after some rearranging, we can write the x-momentum and z-momentum equations for the general case as:

x-Momentum

$$(bf'')' + m_1 ff'' - m_2(f')^2 - m_5 f'g' + m_6 f''g - m_8(g')^2 + m_{11}$$
$$= m_{10}\left(f' \frac{\partial f'}{\partial x_1} - f'' \frac{\partial f}{\partial x_1}\right) + m_7\left(g' \frac{\partial f'}{\partial x_2} - f'' \frac{\partial g}{\partial x_2}\right) \tag{2.25}$$

z-Momentum

$$(bq'')' + m_1 fg'' - m_4 f'g' - m_3 (g')^2 + m_6 gg'' - m_9 (f')^2 + m_{12}$$

$$= m_{10}\left(f' \frac{\partial g'}{\partial x_1} - g'' \frac{\partial f}{\partial x_1}\right) + m_7 \left(g' \frac{\partial g'}{\partial x_2} - g'' \frac{\partial g}{\partial x_2}\right) \qquad (2.26)$$

and their boundary conditions as

$$\eta = 0, \quad f = f' = g = g' = 0, \quad \eta = \eta_\infty, \quad f' = 1, \quad g' = w_e/u_{ref} \qquad (2.27)$$

Here primes denote differentiation with respect to η, and

$$f' = u/u_e, \quad g' = w/u_{ref}, \quad b = 1 + \varepsilon_m^+, \quad \varepsilon_m^+ = \varepsilon_m/\nu \qquad (2.28)$$

The coefficients m_1 to m_{12} are given by

$$m_1 = \frac{1}{2}\left(1 + \frac{s_1}{u_e}\frac{\partial u_e}{\partial s_1}\right) - s_1 K_2, \qquad m_2 = \frac{s_1}{u_e}\frac{\partial u_e}{\partial s_1}, \qquad m_3 = 0$$

$$m_4 = -s_1 K_2, \qquad m_5 = \frac{u_{ref}}{u_e}\frac{s_1}{u_e h_2}\frac{\partial u_e}{\partial x_2} - s_1 K_1$$

$$m_6 = \frac{u_{ref}}{u_e}\left[\frac{1}{2}\left(\frac{\partial s_1}{h_2 \partial x_2} - \frac{s_1}{u_e}\frac{\partial u_e}{h_2 \partial x_2}\right) - s_1 K_2\right], \qquad m_7 = \frac{u_{ref}}{u_e}\frac{s_1}{h_2}$$

$$m_8 = s_1 K_2 \left(\frac{u_{ref}}{u_e}\right)^2, \qquad m_9 = s_1 K_1 \left(\frac{u_e}{u_{ref}}\right), \qquad m_{10} = \frac{s_1}{h_1} \qquad (2.29)$$

$$m_{11} = s_1\left[\frac{1}{u_e}\frac{\partial u_e}{\partial s_1} + \frac{w_e}{u_e}\left(\frac{1}{u_e}\frac{\partial u_e}{h_2 \partial x_2} + K_2 \frac{w_e}{u_e} - K_1\right)\right]$$

$$m_{12} = \frac{u_e}{u_{ref}}\left[\frac{s_1}{u_e}\frac{\partial w_e}{\partial s_1} + \left(\frac{w_e}{u_e}\right)\frac{s_1}{u_e}\frac{\partial w_e}{h_2 \partial x_2} + s_1 K_1 - s_1 K_2 \frac{w_e}{u_e}\right]$$

To transform the <u>streamwise attachment-line</u> flow equations and their boundary conditions, (2.8) to (2.11), we define:

$$uh_2 = \frac{\partial \psi}{\partial y}, \qquad h_1 w_z = \frac{\partial \phi}{\partial y} \qquad (2.30a)$$

$$v = -\frac{1}{h_1 h_2}\left(\frac{\partial \psi}{\partial x_1} + h_2 \phi\right) \tag{2.30b}$$

with ψ and ϕ still given by (2.24). With these variables, the streamwise attachment-line equations in the transformed coordinates can be written as

$$(bf'')' + m_1 ff'' - m_2 (f')^2 + m_6 f''g + m_{11} = m_{10}\left(f' \frac{\partial f'}{\partial x_1} - f'' \frac{\partial f}{\partial x_1}\right) \tag{2.31}$$

$$(bg'')' + m_1 fg'' - m_4 f'g' - m_3 (g')^2 + m_6 gg'' - m_9 (f')^2 + m_{12} = m_{10}\left(f' \frac{\partial g'}{\partial x_1} - g'' \frac{\partial f}{\partial x_1}\right) \tag{2.32}$$

The boundary conditions and the coefficients m_1 to m_{12} are the same as those in (2.27) and in (2.29) except now

$$\eta = \eta_\infty \qquad g' = w_{ze}/u_{ref} \tag{2.33a}$$

$$m_3 = \frac{s_1}{h_2}\frac{u_{ref}}{u_e}, \quad m_6 = m_3, \quad m_9 = \frac{u_e}{u_{ref}} s_1 \frac{\partial K_1}{h_2 \partial x_2}, \quad m_{11} = \frac{s_1}{u_e}\frac{\partial u_e}{\partial s_1}$$

$$m_{12} = \frac{u_e}{u_{ref}}\left[\frac{s_1}{u_e}\frac{\partial w_{ze}}{\partial s_1} + s_1\left(\frac{w_{ze}}{u_e}\right)^2 - s_1 K_2\left(\frac{w_{ze}}{u_e}\right) + s_1 \frac{\partial K_1}{h_2 \partial x_2}\right] \tag{2.33b}$$

The governing equations for the initial conditions normal to the streamwise attachment-line flow are given by the two-dimensional flat-plate equations, which in terms of transformed variables are

$$(bf'')' + \frac{1}{2} ff'' = m_7\left(g' \frac{\partial f'}{\partial x_2} - f'' \frac{\partial g}{\partial x_2}\right) \tag{2.34}$$

$$(bg'')' + \frac{1}{2} fg'' = m_7\left(g' \frac{\partial g'}{\partial x_2} - g'' \frac{\partial g}{\partial x_2}\right) \tag{2.35}$$

For these equations, the boundary conditions are given by (2.27).

In terms of transformed variables, the <u>algebraic eddy-viscosity formulas</u> as given by (2.13) to (2.15) become

$$(\varepsilon_m^+)_i = \left\{0.4\eta[1 - \exp(-y^+/26)]\right\}^2 \left\{R_s \left[(f'')^2 + \left(\frac{u_{ref}}{u_e} g''\right)^2\right]\right\}^{1/2} \tag{2.36}$$

$$(\varepsilon_m^+)_o = 0.0168 R_s^{1/2} \left\{\left[1 + \left(\frac{w_e}{u_e}\right)^2\right]^{1/2} \eta_\infty - \int_0^{\eta_e} \left[f'^2 + \left(\frac{u_{ref}}{u_e} g'\right)^2\right]^{1/2} d\eta\right\}$$

Here (2.37)

$$R_s = \frac{u_e s_1}{\nu} \qquad y^+ = \eta R_s^{1/4} \left[f_w''^2 + \left(\frac{u_{ref}}{u_e} g_w''\right)^2\right]^{1/4} \tag{2.38}$$

3.0 NUMERICAL METHOD

We use the Box method to solve the governing equations. This is a two-point finite-difference method developed by Keller and Cebeci. So far this method has been applied to two-dimensional flows as well as three-dimensional flows and has been found to be efficient and accurate. Descriptions of this method have been presented in a series of papers and reports, and a detailed presentation is contained in a forthcoming book by Cebeci and Bradshaw[6]. For completeness we shall present a brief description of this method in application to our equations. At first we shall discuss the solution of the streamwise attachment-line equations, (2.31) and (2.32), and then the solution of the full three-dimensional flow equations as given by (2.25) and (2.26).

3.1 Difference Equations for the Streamwise Attachment-Line Equations

According to the Box method, we first reduce the equations (2.31), (2.32), (2.27) and (2.33a) into a system of six first-order equations by introducing new dependent variables $u(x_1, x_2, \eta)$, $v(x_1, x_2, \eta)$, $w(x_1, x_2, \eta)$ and $t(x_1, x_2, \eta)$. Equations (2.31) and (2.32) then can be written as

$$f' = u \tag{3.1a}$$

$$u' = v \tag{3.1b}$$

$$g' = w \tag{3.1c}$$

$$w' = t \tag{3.1d}$$

$$(bv)' + m_1 fv - m_2 u^2 + m_6 gv + m_{11} = m_{10}\left(u\frac{\partial u}{\partial x_1} - v\frac{\partial f}{\partial x_1}\right) \tag{3.1e}$$

$$(bt)' + m_1 ft - m_4 uw - m_3 w^2 + m_6 gt - m_9 u^2 + m_{12} = m_{10}\left(u\frac{\partial w}{\partial x_1} - t\frac{\partial f}{\partial x_1}\right) \tag{3.1f}$$

The boundary conditions (2.27) and (2.33a) become

$$\eta = 0 \qquad f = g = u = w = 0 \tag{3.2a}$$

$$\eta = \eta_\infty \qquad u = 1 \qquad w = w_{ze}/u_{ref} \tag{3.2b}$$

We next consider the net rectangle shown in Figure 2 and denote the net points by

$$(x_1)_0 = 0 \qquad (x_1)_n = (x_1)_{n-1} + k_n \qquad n = 1, 2, \ldots, N$$

$$\eta_0 = 0 \qquad \eta_j = \eta_{j-1} + h_j \qquad j = 1, 2, \ldots, J$$

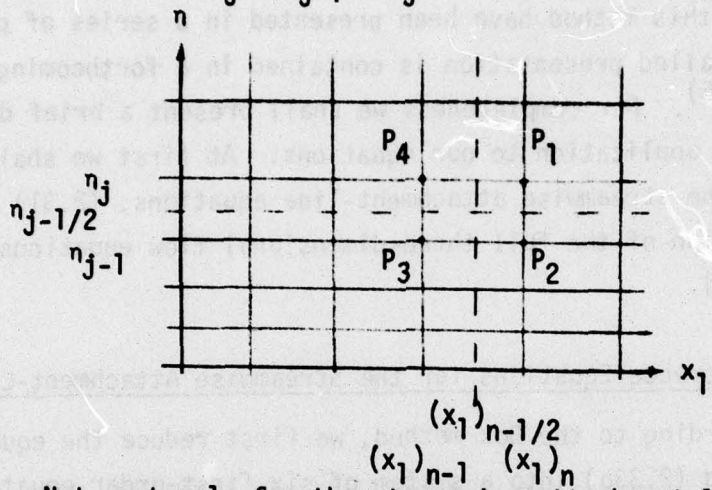

Figure 2. Net rectangle for the streamwise-attachment-line equations

We approximate the quantities (f, u, v, g, w, t) at points $[(x_1)_n, \eta_j]$ of the net by functions denoted by $(f_j^n, u_j^n, v_j^n, g_j^n, w_j^n, t_j^n)$. We also employ the notation for points and quantities midway between net points and for any net function s_j^n:

$$(x_1)_{n-1/2} = \tfrac{1}{2}[(x_1)_n + (x_1)_{n-1}] \qquad \eta_{j-1/2} = \tfrac{1}{2}(\eta_j + \eta_{j-1})$$

$$s_j^{n-1/2} = \tfrac{1}{2}(s_j^n + s_j^{n-1}) \qquad s_{j-1/2} = \tfrac{1}{2}(s_j^n + s_{j-1}^n) \tag{3.3}$$

The difference equations which are to approximate (3.1) are formulated by considering one mesh rectangle as in Figure 2. We approximate (3.1a, b, c, d) using centered difference quotients and average them about the midpoint $[(x_1)_n, \eta_{j-1/2}]$ of the segment P_1P_2.

$$h_j^{-1}(f_j^n - f_{j-1}^n) = u_{j-1/2}^n \tag{3.4a}$$

$$h_j^{-1}(u_j^n - u_{j-1}^n) = v_{j-1/2}^n \tag{3.4b}$$

$$h_j^{-1}(g_j^n - g_{j-1}^n) = w_{j-1/2}^n \tag{3.4c}$$

$$h_j^{-1}(w_j^n - w_{j-1}^n) = t_{j-1/2}^n \tag{3.4d}$$

Similarly, (3.1e,f) are approximated by centering them about the midpoint $(x_1)_{n-1/2}, \eta_{j-1/2}$ of the rectangle $P_1P_2P_3P_4$. This gives:

$$h_j^{-1}[(bv)_j^n - (bv)_{j-1}^n] + (m_1^n + \alpha_n)(fv)_{j-1/2}^n - (m_2^n + \alpha_n)(u^2)_{j-1/2}^n$$
$$+ m_6^n(gv)_{j-1/2}^n + \alpha_n[v_{j-1/2}^{n-1}f_{j-1/2}^n - f_{j-1/2}^{n-1}v_{j-1/2}^n]$$
$$= R_{j-1/2}^{n-1} - m_{11}^n \tag{3.4e}$$

$$h_j^{-1}[(bt)_j^n - (bt)_{j-1}^n] + (m_1^n + \alpha_n)(ft)_{j-1/2}^n - (m_4^n + \alpha_n)(uw)_{j-1/2}^n$$
$$- m_3^n(w^2)_{j-1/2}^n + m_6^n(gt)_{j-1/2}^n - m_9^n(u^2)_{j-1/2}^n$$
$$+ \alpha_n[w_{j-1/2}^{n-1}u_{j-1/2}^n - u_{j-1/2}^{n-1}w_{j-1/2}^n + t_{j-1/2}^{n-1}f_{j-1/2}^n$$
$$- f_{j-1/2}^{n-1}t_{j-1/2}^n] = T_{j-1/2}^{n-1} - m_{12}^n \tag{3.4f}$$

Here

$$R_{j-1/2}^{n-1} = \alpha_n[(fv)_{j-1/2}^{n-1} - (u^2)_{j-1/2}^{n-1}] - [h_j^{-1}\{(bv)_j^{n-1} - (bv)_{j-1}^{n-1}\} + m_1^{n-1}(fv)_{j-1/2}^{n-1}$$
$$- m_2^{n-1}(u^2)_{j-1/2}^{n-1} + m_6^{n-1}(gv)_{j-1/2}^{n-1} + m_{11}^{n-1}] \tag{3.5a}$$

$$T_{j-1/2}^{n-1} = \alpha_n[(ft)_{j-1/2}^{n-1} - (uw)_{j-1/2}^{n-1}] - [h_j^{-1}\{(bt)_j^{n-1} - (bt)_{j-1}^{n-1}\} + m_1^{n-1}(ft)_{j-1/2}^{n-1}$$
$$- m_4^{n-1}(uw)_{j-1/2}^{n-1} - m_3^{n-1}(w^2)_{j-1/2}^{n-1} + m_6^{n-1}(gt)_{j-1/2}^{n-1}$$
$$- m_9^{n-1}(u^2)_{j-1/2}^{n-1} + m_{12}^{n-1}] \tag{3.5b}$$

$$\alpha_n \equiv \frac{m_{10}^{n-1/2}}{(x_1)_n - (x_1)_{n-1}} \tag{3.5c}$$

3.2 Difference Equations for the Full Three-Dimensional Equations

The difference equations for the full three-dimensional equations, as given by (2.25) and (2.26), are again expressed in terms of a first-order system. With the definitions given by (3.1a) to (3.1d), they are written as

$$(bv)' + m_1 fv - m_2 u^2 - m_5 uw + m_6 gv - m_8 w^2 + m_{11}$$

$$= m_{10}\left(u\frac{\partial u}{\partial x_1} - v\frac{\partial f}{\partial x_1}\right) + m_7\left(w\frac{\partial u}{\partial x_2} - v\frac{\partial g}{\partial x_2}\right) \tag{3.6a}$$

$$(bt)' + m_1 ft - m_4 uw - m_3 w^2 + m_6 gt - m_9 u^2 + m_{12}$$

$$= m_{10}\left(u\frac{\partial w}{\partial x_1} - t\frac{\partial f}{\partial x_1}\right) + m_7\left(w\frac{\partial w}{\partial x_2} - t\frac{\partial g}{\partial x_2}\right) \tag{3.6b}$$

Their boundary conditions, (2.27), become:

$$\eta = 0 \qquad f = g = u = w = 0 \tag{3.7a}$$

$$\eta = \eta_\infty \qquad u = 1, \qquad w = w_e/u_{ref} \tag{3.7b}$$

The difference equations for (3.1a) to (3.1d) are the same as those given by (3.4a) to (3.4d): they are written for the midpoint $[(x_1)_n, (x_2)_i, \eta_{j-1/2}]$ of the net cube shown in Figure 3; that is,

$$h_j^{-1}(f_j^{n,i} - f_{j-1}^{n,i}) = u_{j-1/2}^{n,i}, \quad h_j^{-1}(u_j^{n,i} - u_{j-1}^{n,i}) = v_{j-1/2}^{n,i}, \quad \text{etc.}$$

The difference equations which are to approximate (3.6a,b) are rather lengthy. To illustrate the difference equations for these two equations, we consider the following model equation

$$(bv)' + m_1 fv + m_{11} = m_{10}\, u\frac{\partial u}{\partial x_1} + m_7 w\frac{\partial u}{\partial x_2} \tag{3.8}$$

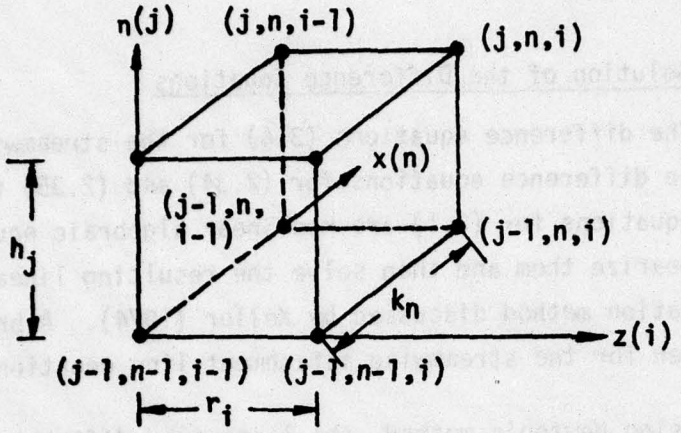

Figure 3. Net cube for the difference equations for three-dimensional flows.

The difference equations for (3.8) are:

$$h_j^{-1}[(\overline{bv})_j - (\overline{bv})_{j-1}] + (m_1)_{j-1/2}^{n-1/2}(\overline{fv})_{j-1/2} + (m_{11})_{j-1/2}^{n-1/2}$$

$$= (m_{10})_{i-1/2}^{n-1/2}\,\overline{u}_{j-1/2}\,\frac{\overline{u}_n - \overline{u}_{n-1}}{k_n} + (m_7)_{i-1/2}^{n-1/2}\,\overline{w}_{j-1/2}\,\frac{\overline{u}_i - \overline{u}_{i-1}}{r_i} \tag{3.9}$$

Here, for example,

$$\begin{aligned}
\overline{v}_j &= \tfrac{1}{4}\,(v_j^{n,i} + v_j^{n,i-1} + v_j^{n-1,i-1} + v_j^{n-1,i}) \\
\overline{u}_n &= \tfrac{1}{4}\,(u_j^{n,i} + u_j^{n,i-1} + u_{j-1}^{n,i} + u_{j-1}^{n,i-1}) \\
\overline{u}_i &= \tfrac{1}{4}\,(u_j^{n,i} + u_j^{n-1,i} + u_{j-1}^{n,i} + u_{j-1}^{n-1,i}) \\
(m_1)_{i-1/2}^{n-1/2} &= \tfrac{1}{4}\,[(m_1)_i^n + (m_1)_{i-1}^n + (m_1)_i^{n-1} + (m_1)_{i-1}^{n-1}]
\end{aligned} \tag{3.10}$$

and

$$z_0 = 0 \qquad z_i = z_{i-1} + r_i \qquad i = 1, 2, \ldots, I \tag{3.11}$$

3.3 Solution of the Difference Equations

The difference equations (3.4) for the streamwise attachment-line flow and the difference equations for (2.34) and (2.35) together with the difference equations for (3.1) are nonlinear algebraic equations. We use Newton's metho to linearize them and then solve the resulting linear system by the block-elimination method discussed by Keller (1974). A brief description of it will be given for the streamwise attachment-line equations.

Using Newton's method, the linearized difference equations for the system given by (3.4) and (3.2) are:

$$\delta f_j - \delta f_{j-1} - \frac{h_j}{2}(\delta u_j + \delta u_{j-1}) = (r_i)_j \tag{3.12a}$$

$$\delta u_j - \delta u_{j-1} - \frac{h_j}{2}(\delta v_j + \delta v_{j-1}) = (r_2)_j \tag{3.12b}$$

$$\delta g_j - \delta g_{j-1} - \frac{h_j}{2}(\delta w_j + \delta w_{j-1}) = (r_3)_j \tag{3.12c}$$

$$\delta w_j - \delta w_{j-1} - \frac{h_j}{2}(\delta t_j + \delta t_{j-1}) = (r_4)_j \tag{3.12d}$$

$$(\zeta_1)_j \delta v_j + (\zeta_2)_j \delta v_{j-1} + (\zeta_3)_j \delta f_j + (\zeta_4)_j \delta f_{j-1} + (\zeta_5)_j \delta u_j + (\zeta_6)_j \delta u_{j-1} + (\zeta_7)_j \delta g_j + (\zeta_8)_j \delta g_{j-1} = (r_5)_j \tag{3.12e}$$

$$(\beta_1)_j \delta t_j + (\beta_2)_j \delta t_{j-1} + (\beta_3)_j \delta f_j + (\beta_4)_j \delta f_{j-1} + (\beta_5)_j \delta w_j + (\beta_6)_j \delta w_{j-1} + (\beta_7)_j \delta u_j + (\beta_8)_j \delta u_{j-1} + (\beta_9)_j \delta g_j + (\beta_{10})_j \delta g_{j-1} = (r_6)_j \tag{3.12f}$$

Here we have dropped the superscripts n, i and have defined $(r_k)_j$, $(\zeta_k)_j$ and $(\beta_k)_j$ by

$$\begin{aligned} (r_1)_j &= f_{j-1} - f_j + h_j u_{j-1/2}, & (r_2)_j &= u_{j-1} - u_j + h_j v_{j-1/2}, \\ (r_3)_j &= g_{j-1} - g_j + h_j - w_{j-1/2}, & (r_4)_j &= w_{j-1} - w_j + h_j t_{j-1/2} \end{aligned} \tag{3.13}$$

$$(r_5)_j = R^{n-1}_{j-1/2} - m^n_{11} - [(bv)'_{j-1/2} + (m_1 + \alpha_n)(fv)_{j-1/2} - (m_2 + \alpha_n)(u^2)_{j-1/2}$$
$$+ m_6(gv)_{j-1/2} + \alpha_n (v^{n-1}_{j-1/2} f_{j-1/2} - f^{n-1}_{j-1/2} v_{j-1/2})]$$

$$(r_6)_j = T^{n-1}_{j-1/2} - m_{12} - [(bt)'_{j-1/2} + (m_1 + \alpha_n)(ft)_{j-1/2} - (m_4 + \alpha_n)(uw)_{j-1/2}$$
$$- m_3(w^2)_{j-1/2} + m_6(gt)_{j-1/2} - m_9(u^2)_{j-1/2}$$
$$+ \alpha_n(w^{n-1}_{j-1/2} u_{j-1/2} - u^{n-1}_{j-1/2} w_{j-1/2} + t^{n-1}_{j-1/2} f_{j-1/2}$$
$$- f^{n-1}_{j-1/2} t_{j-1/2})] \qquad (3.13)$$

$$(\zeta_1)_j = \frac{b_j}{h_j} + \frac{1}{2}(m_1 + \alpha_n) f_j - \frac{\alpha_n}{2} f^{n-1}_{j-1/2} + \frac{1}{2} m_6 g_j \qquad (3.14a)$$

$$(\zeta_2)_j = -\frac{b_{j-1}}{h_j} + \frac{1}{2}(m_1 + \alpha_n) f_{j-1} + \frac{\alpha_n}{2} f^{n-1}_{j-1/2} + \frac{1}{2} m_6 g_{j-1} \qquad (3.14b)$$

$$(\zeta_3)_j = \frac{1}{2}(m_1 + \alpha_n) v_j + \frac{\alpha_n}{2} v^{n-1}_{j-1/2} \qquad (3.14c)$$

$$(\zeta_4)_j = \frac{1}{2}(m_1 + \alpha_n) v_{j-1} + \frac{\alpha_n}{2} v^{n-1}_{j-1/2} \qquad (3.14d)$$

$$(\zeta_5)_j = -(m_2 + \alpha_n) u_j \qquad (3.14e)$$

$$(\zeta_6)_j = -(m_2 + \alpha_n) u_{j-1} \qquad (3.14f)$$

$$(\zeta_7)_k = \frac{1}{2} m_6 v_j, \qquad (\zeta_8)_j = \frac{m_6}{2} v_{j-1} \qquad (3.14g)$$

$$(\beta_1)_j = (\zeta_1)_j, \qquad (\beta_2)_j = (\zeta_2)_j, \qquad (\beta_3)_j = \frac{1}{2}(m_1 + \alpha_n) t_j + \frac{\alpha_n}{2} t^{n-1}_{j-1/2}$$
$$(\beta_4)_j = \frac{1}{2}(m_1 + \alpha_n) t_{j-1} + \frac{\alpha_n}{2} t^{n-1}_{j-1/2},$$
$$(\beta_5)_j = -\frac{1}{2}(m_4 + \alpha_n) u_j - m_3 w_j - \frac{\alpha_n}{2} u^{n-1}_{j-1/2}$$
$$(\beta_6)_j = -\frac{1}{2}(m_4 + \alpha_n) u_{j-1} - m_3 w_{j-1} - \frac{\alpha_n}{2} u^{n-1}_{j-1/2} \qquad (3.15)$$

$$(\beta_7)_j = -\frac{1}{2}(m_4 + \alpha_n)w_j - m_9 u_j + \frac{\alpha_n}{2} w_{j-1/2}^{n-1}$$

$$(\beta_8)_j = -\frac{1}{2}(m_4 + \alpha_n)w_{j-1} - m_9 u_{j-1} + \frac{\alpha_n}{2} w_{j-1/2}^{n-1}$$

$$(\beta_9)_j = \frac{1}{2} m_6 t_j, \qquad (\beta_{10})_j = \frac{m_6}{2} t_{j-1} \tag{3.15}$$

The boundary conditions become

$$\delta f_0 = \delta g_0 = \delta u_0 = \delta w_0 = 0 \quad , \quad \delta u_J = \delta w_J = 0 \tag{3.16}$$

The solution of the linear system given by (3.12) and (3.16) is obtained by using the block elimination method. According to this method, the system is written as

$$\mathbf{A}\, \underset{\sim}{\delta} = \underset{\sim}{r} \tag{3.17}$$

Here

$$\mathbf{A} = \begin{bmatrix} A_0 & C_0 & & & & \\ B_1 & A_1 & C_1 & & & \\ & B_j & A_j & C_j & & \\ & & B_{J-1} & A_{J-1} & C_{J-1} & \\ & & & B_J & A_J & \end{bmatrix} \qquad \underset{\sim}{\delta} = \begin{bmatrix} \underset{\sim}{\delta}_0 \\ \underset{\sim}{\delta}_1 \\ \vdots \\ \underset{\sim}{\delta}_j \\ \vdots \\ \underset{\sim}{\delta}_J \end{bmatrix}$$

$$\underset{\sim}{r} = \begin{bmatrix} \underset{\sim}{r}_1 \\ \underset{\sim}{r}_2 \\ \underset{\sim}{r}_j \\ \underset{\sim}{r}_J \end{bmatrix} \qquad \underset{\sim}{r}_j \equiv \begin{bmatrix} (r_1)_j \\ (r_2)_j \\ (r_3)_j \\ (r_4)_j \\ (r_5)_j \\ (r_6)_j \end{bmatrix} \qquad \underset{\sim}{\delta}_j \equiv \begin{bmatrix} \delta f_j \\ \delta u_j \\ \delta v_j \\ \delta g_j \\ \delta w_j \\ \delta t_j \end{bmatrix}$$

The A_j, B_j, C_j in $\mathbf{A}$ denote 6 x 6 matrices. The solution of (3.17) is obtained by the procedure described in reference 6.

4.0 PRELIMINARY RESULTS

In order to check the method, we have considered the calculation of boundary-layer development on a body represented analytically by

$$y = f(x,z) = B\left[1 - \left(\frac{x}{L}\right)^2\right]^{1/2}\left[1 - \left(\frac{z}{H}\right)^2\right]^{1/2} \qquad (4.1)$$

This is a double-elliptic ship having round edges except for the shape corners at $x = \pm L$ and $z = \pm H$ as shown in figure 4. The potential-flow solutions for the body of L:H:B = 1:0.1:0.125 were obtained from the Douglas-Neumann

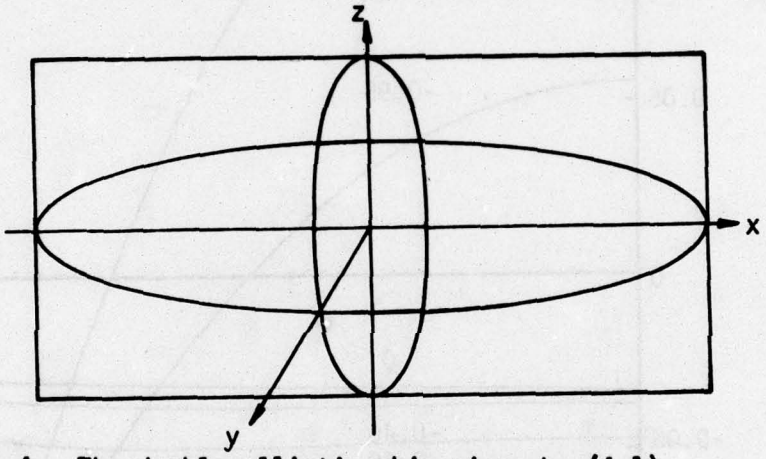

Figure 4. The double-elliptic ship given by (4.1).

computer program for three-dimensional flows (see figure 5). To get the solutions, 120 control elements on the surface were used, 12 along the x-direction and 10 along the z-direction.

Before we describe our boundary-layer calculations for the ship given by (4.1), it is useful to discuss the pressure distribution for this body. As can be seen from figure 5, the streamwise pressure gradient is initially favorable in the bow region and then adverse up to the midpoint of the body. This is followed by a region of favorable pressure and then by a sharp adverse pressure gradient very close to the stern. The crosswise pressure gradient varies in a more complex manner. Near the bow, the pressure decreases as z increases. As the flow moves downstream, the location of the minimum pressure moves up and finally reaches the water surface. This implies that the cross-flow will reverse its sign a number of times. As a result, in some regions we

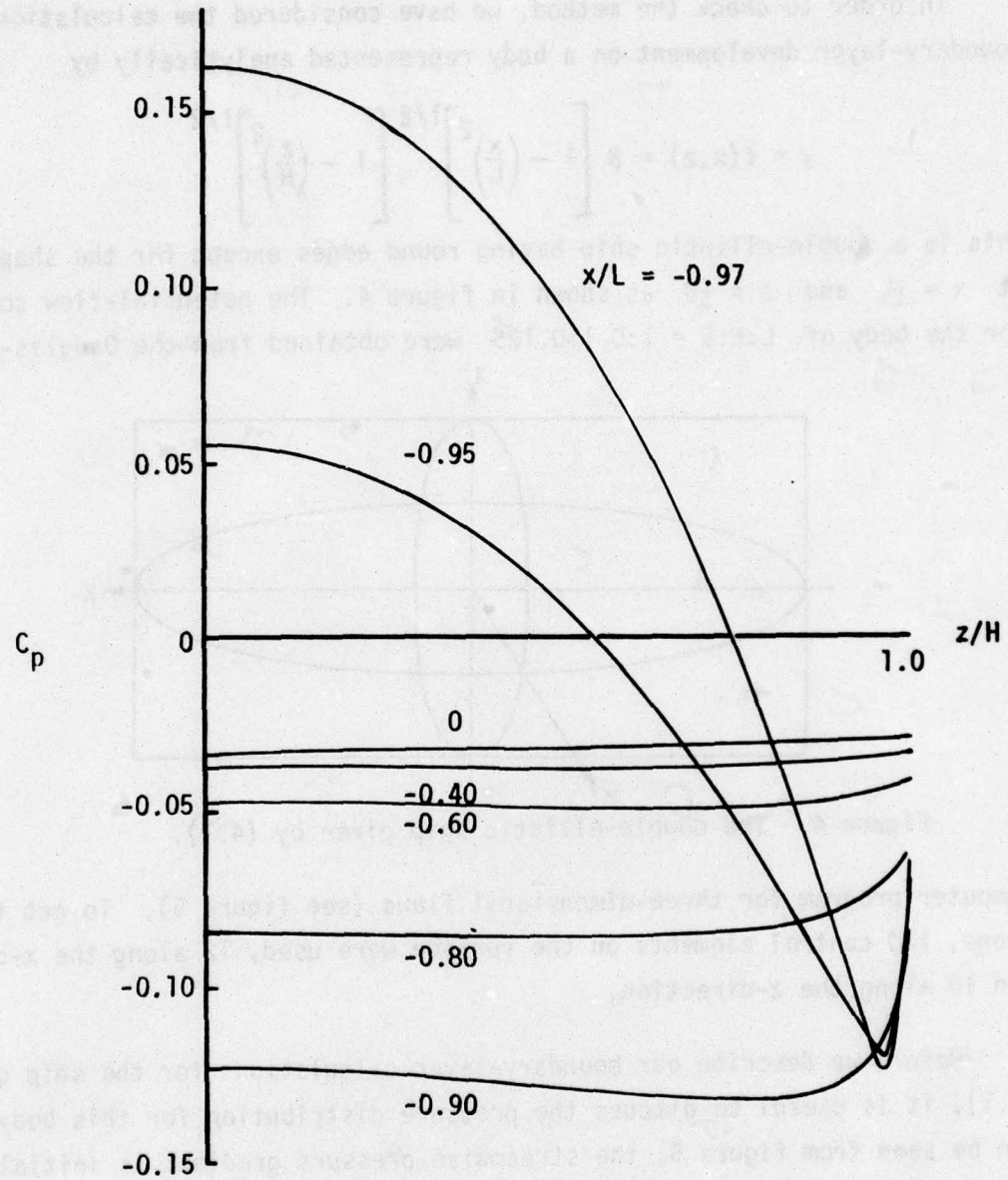

Figure 5. Pressure distribution for a double-elliptic ship form of 1:0.1:0.125.

may expect the cross-over type of the crossflow profiles (i.e., where the direction of the crossflow changes across the boundary layer). This conclusion is drawn from considering the pressure gradients only. The real situation is more complicated because, in addition, there are the upstream effects and the curvature effects on the flow characteristics.

The boundary-layer computation starts from $x_1/L = -0.97$. The region between this point and the bow is not considered for two reasons: first, the pressure distribution in this region is not available from the potential-flow computer program and second, the sharp corner at $x_1/L = -1.0$ and $z/H = 1.0$ implies an infinite curvature and, hence, the boundary-layer assumptions are no longer valid in that region. In our boundary-layer calculations, we have used 32 points along the x_1-direction and 12 points along the x_2-direction. In the normal direction, we have taken approximately 40 points. The flow was assumed to be laminar at first and then was specified to be turbulent at the third (x_1/L)-station, namely at $x_1/L = -0.925$.

Some of the computed results for $R_L = 10^7$ are shown in figures 6 to 10. Figures 6, 7, and 8 show the streamwise variation of the local skin-friction coefficient, the shape factor, and the Reynolds number based on the momentum thickness for $z/H = 0$, 0.1, 0.2, and 0.3, respectively. Figures 9 and 10 show some of the typical streamwise and crosswise velocity profiles along $z/H = 0.3$. In these two figures, the profiles for $z/H = 0.0$ correspond to the streamwise attachment solutions $(z/H = 0)$. We see from figure 3 that the flow along the attachment line separates at approximately $x/L = 0.95$, or near the stern, where the pressure gradient is sharply adverse. As z/H increases, the point of separation moves upstream. Along the line, $z/H = 0.3$, the flow separates at about $x/L = 0.80$, where the pressure is almost constant. This unusual behavior results from the crossflow effect. A better marching procedure is required to remedy the situation as is discussed in the next section.

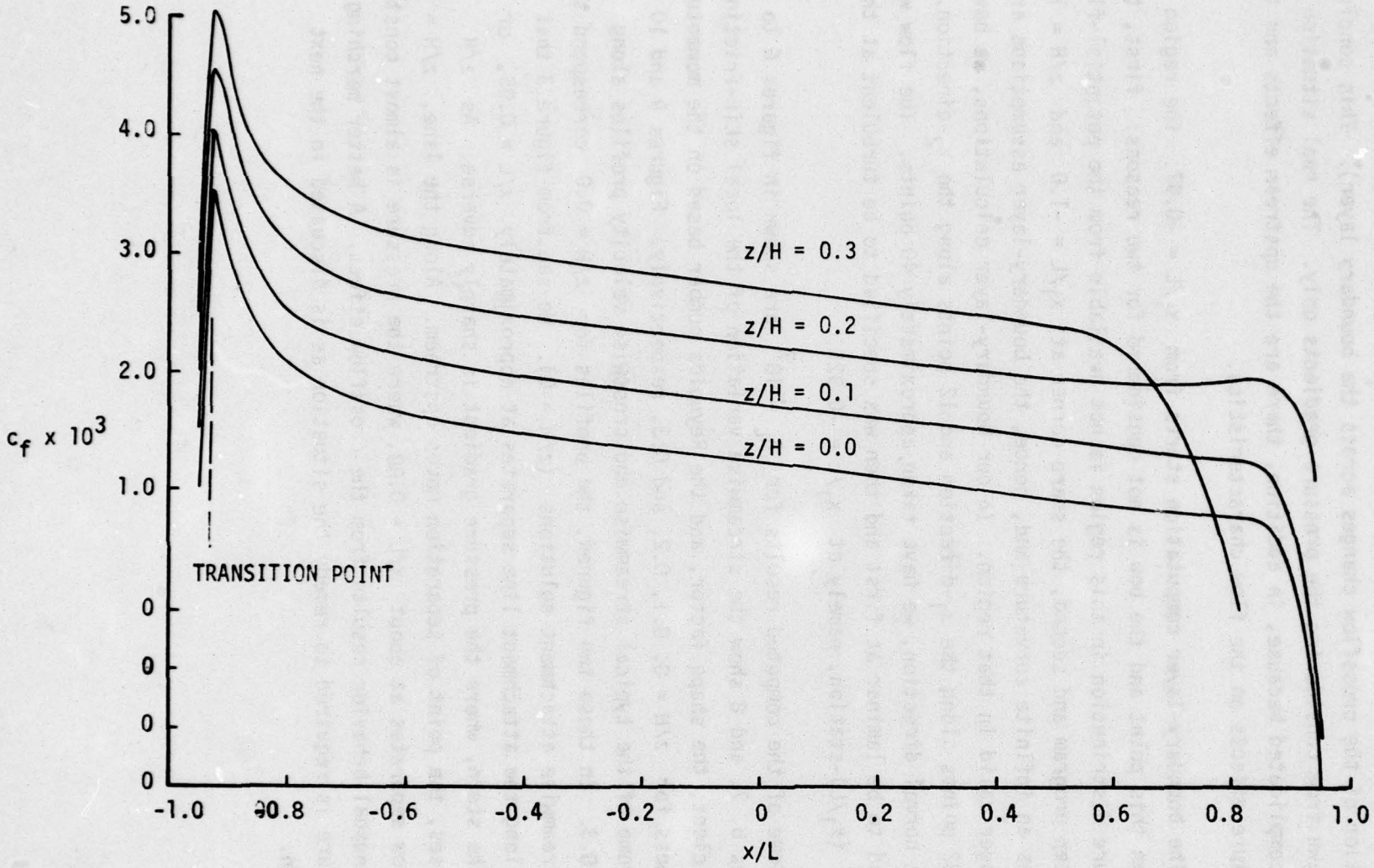

Figure 6. Variation of skin-friction coefficient along the streamwise direction for the double-elliptic ship.

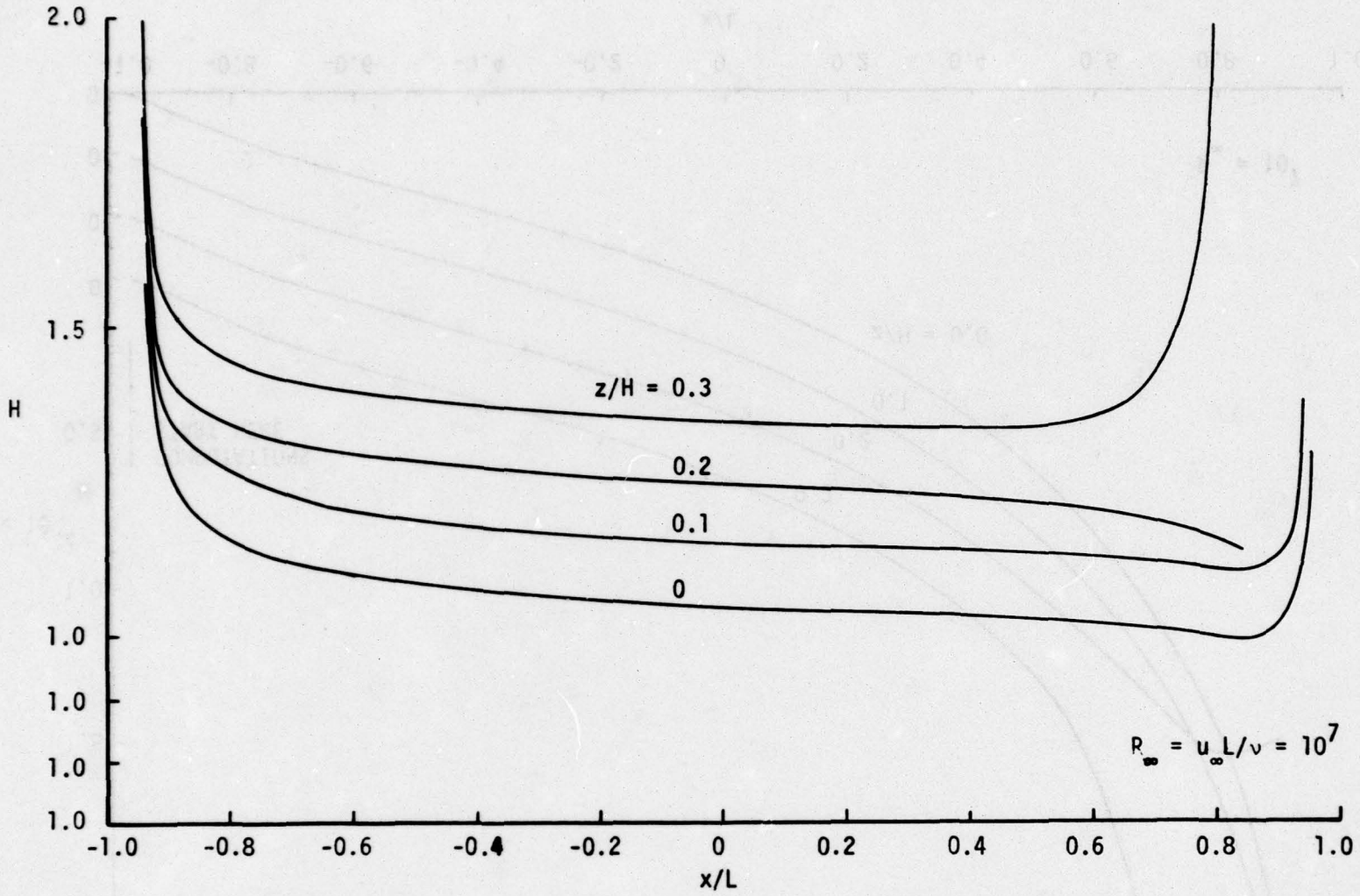

Figure 7. Variation of shape factor H on the streamwise direction.

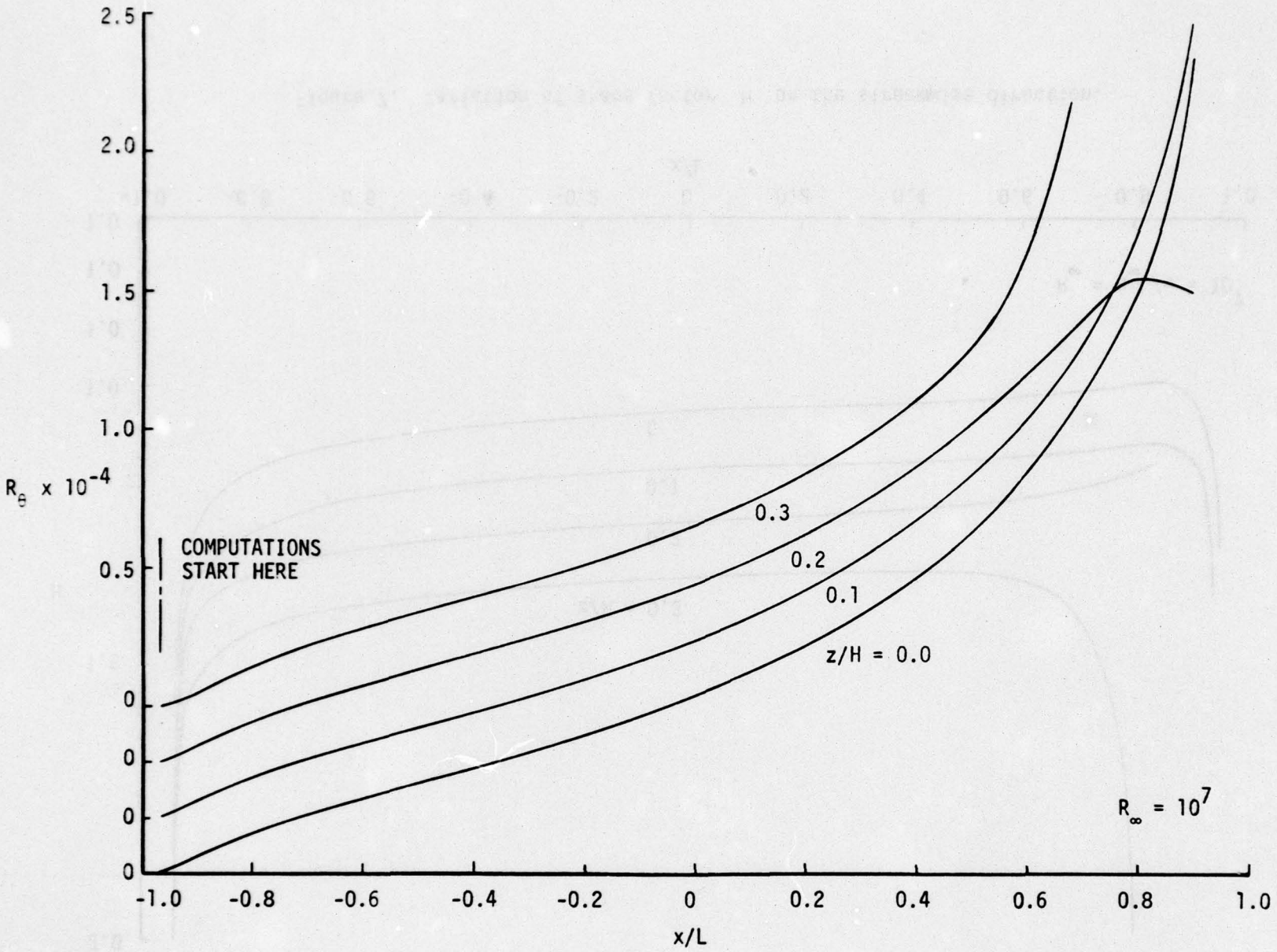

Figure 8. Variation of R_θ along the streamwise direction for the double-elliptic ship.

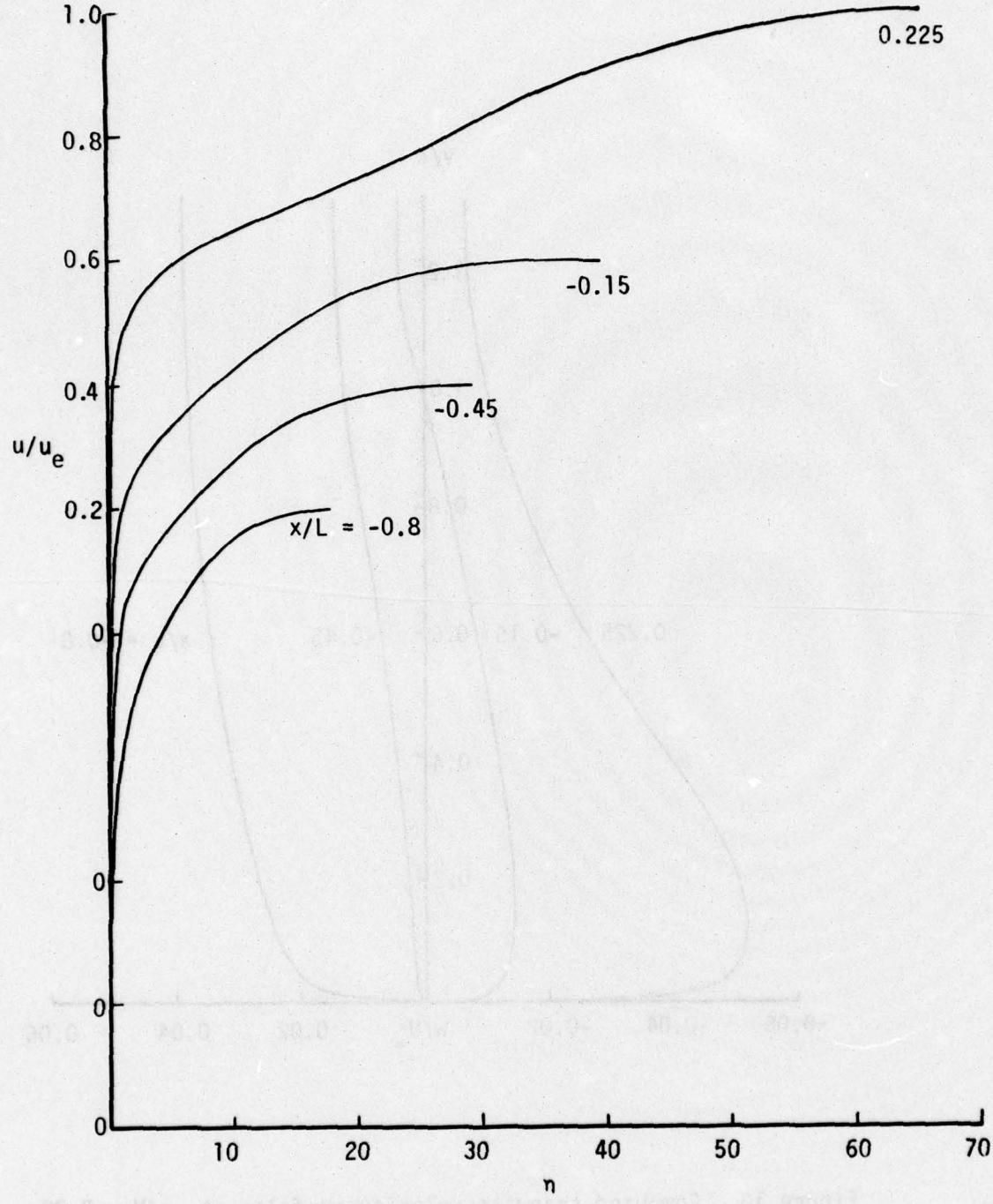

Figure 9. Computed streamwise velocity profiles at z/H = 0.3.

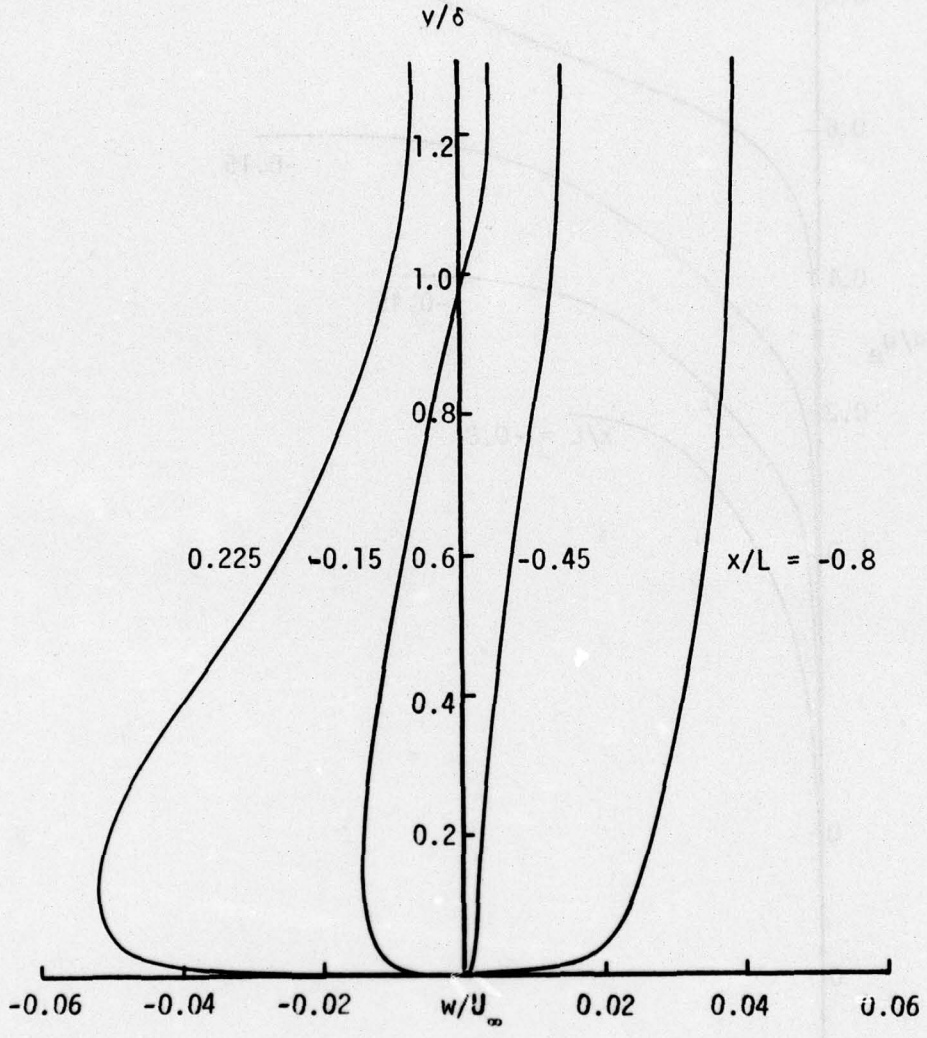

Figure 10. Computed spanwise velocity profiles at z/H = 0.30.

5.0 DISCUSSION

The present effort is one step towards developing a general method for computing three-dimensional boundary layers on ship hulls. Obviously further studies are needed in the following areas:

1. A better numerical procedure for handling the computation of flows in which there are regions of negative crossflow. Our present calculations here and in the related problems[7] demonstrate that in regions of the flow field where there is a significant layer of crossflow opposing the marching direction, oscillations can occur in the generated solution. These are caused by the stability condition on the difference equations which does not permit the correct domain of dependence of the differential equation to be utilized at the particular point being computed.

2. A better coordinate system than the one used in this study is required. As discussed in Section 2.3, a nonorthogonal system is appropriate for ship hulls. Although the governing equations are slightly more complicated than those for an orthogonal system, that complication does not cause any difficulties in their numerical solution. The big advantage of the nonorthogonal system is the control it allows over the coordinate net spacing. In orthogonal systems, a family of surfaces which intersects the hull surface has been selected, the orthogonals are consequently determined and, for some ship hulls, can lead to coordinate nets which are unacceptably sparce at some areas.

These necessary studies indicated above are presently in progress. A recently developed procedure, which looks particularly promising, uses the notation of domain of dependence and follows the characteristics of the locally plane flow. In this procedure, the direction of w at each η_j-grid point is examined and the difference equations formulated accordingly. In addition, the new procedure utilizes a modification of the Box scheme similar to the zig-zag differencing scheme proposed by Krause et al.[8] and successfully used by Cebeci[9] to compute the unsteady flow generated by an impulsively started circular cylinder. The finite-difference equations, with the

zig-zag differencing used to advance in time, have been solved from time $t = 0$ until the time the separation point has moved from the rear of the cylinder to its final steady-state value of $\theta = 106°$. The flow reversal has been accounted for satisfactorily and the calculations extended further in time than many previous studies.

An example of a nonorthogonal coordinate system is given by the intersection of meridian planes and parallel cuts. Consider the hull as given in the usual Cartesian coordinate system, that is, x along the ship axis, y and z in the crossplane (see Figure 11). We select x as one of the coordinates and the polar angle ϕ in the yz-plane as the other coordinate. It is only necessary to define the hull as a family of points in the planes $x = \text{constant}$. Then the data is spline-fitted in each crossplane as y vs ϕ and z vs ϕ, and interpolated for constant values of ϕ. Then another set of spline fits in planes $\phi = \text{constant}$ for y vs x and z vs x completes the definition of the coordinate system. The lines formed by the intersection of the planes $x = \text{constant}$ and $\phi = \text{constant}$ with the hull surface constitute the nonorthogonal coordinate net on the surface, and the third boundary-layer coordinate is taken as the distance normal to the surface in accordance with first-order boundary-layer approximations.

Since the spline-fitting also yields derivatives, the metric coefficients and the geodesic curvatures of the coordinate lines can be calculated by using the formulas given below.

The metric coefficients:

$$h_1^2 = 1 + \left(\frac{\partial z}{\partial x}\right)_\phi^2 + \left(\frac{\partial y}{\partial x}\right)_\phi^2$$

$$h_2^2 = \left(\frac{\partial y}{\partial \phi}\right)_x^2 + \left(\frac{\partial z}{\partial \phi}\right)_x^2$$

The angle between the coordinate lines

$$\cos\theta = \frac{1}{h_1 h_2}\left[\left(\frac{\partial y}{\partial \phi}\right)_x \left(\frac{\partial y}{\partial x}\right)_\phi + \left(\frac{\partial z}{\partial \phi}\right)_x \left(\frac{\partial z}{\partial x}\right)_\phi\right]$$

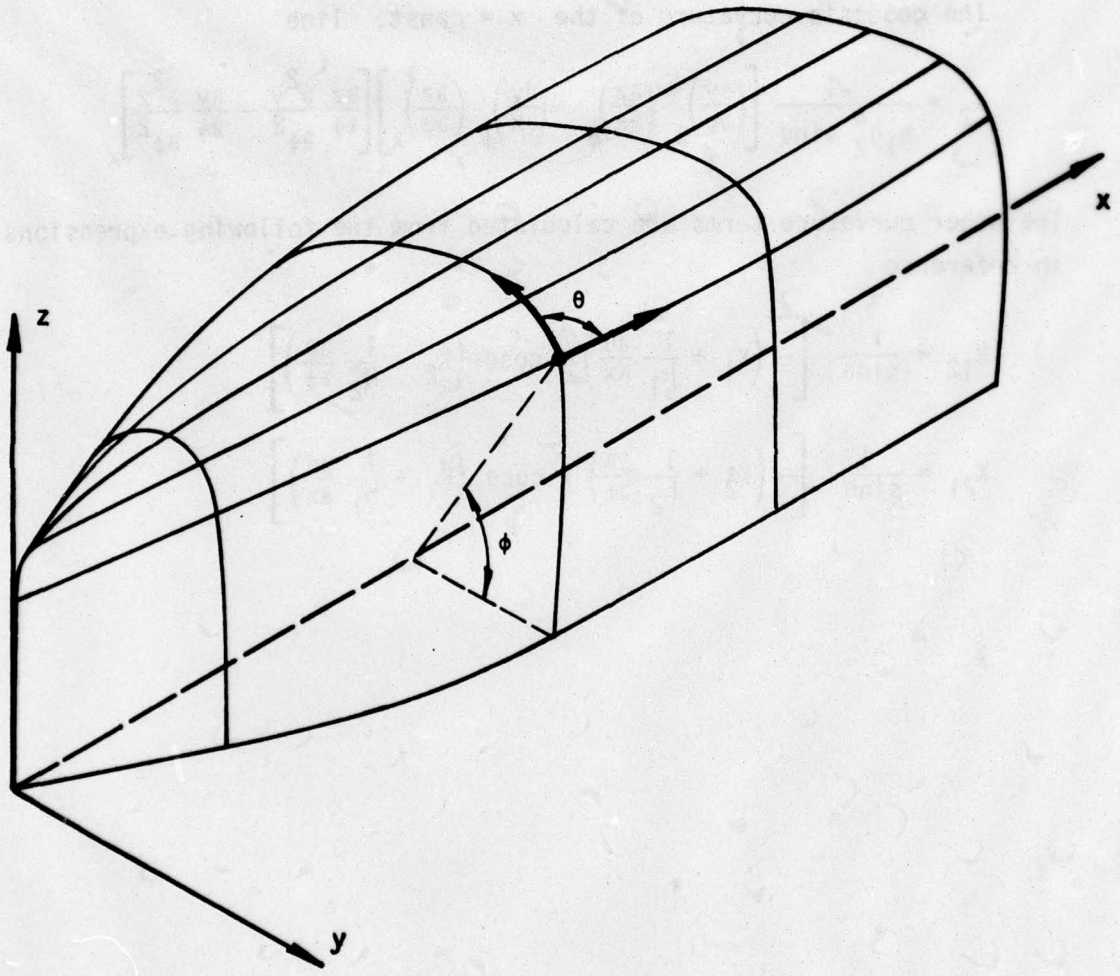

Figure 11. Nonorthogonal coordinate system for the ship hull.

The geodesic curvature of the ϕ = const. line

$$K_1 = \frac{1}{h_1^4 h_2 \sin\theta}\left\{\left[\left(\frac{\partial y}{\partial \phi}\right)_x \left(\frac{\partial z}{\partial x}\right)_\phi - \left(\frac{\partial y}{\partial x}\right)_\phi \left(\frac{\partial z}{\partial \phi}\right)_x\right] \cdot \left(\frac{\partial z}{\partial x}\frac{\partial^2 y}{\partial x^2} - \frac{\partial y}{\partial x}\frac{\partial^2 z}{\partial x^2}\right)_\phi \right.$$

$$\left. + \left[\left(\frac{\partial y}{\partial \phi}\right)_x \left(\frac{\partial^2 y}{\partial x^2}\right)_\phi + \left(\frac{\partial z}{\partial \phi}\right)_x \left(\frac{\partial^2 z}{\partial x^2}\right)_\phi\right]\right\}$$

The geodesic curvature of the x = const. line

$$K_2 = \frac{-1}{h_1 h_2^4 \sin\theta}\left[\left(\frac{\partial y}{\partial \phi}\right)_x \left(\frac{\partial z}{\partial x}\right)_\phi - \left(\frac{\partial y}{\partial x}\right)_\phi \left(\frac{\partial z}{\partial \phi}\right)_x\right]\left[\frac{\partial z}{\partial \phi}\frac{\partial^2 y}{\partial \phi^2} - \frac{\partial y}{\partial \phi}\frac{\partial^2 z}{\partial \phi^2}\right]_x$$

The other curvature terms are calculated from the following expressions given in reference

$$K_{12} = \frac{1}{\sin\theta}\left[-\left(K_1 + \frac{1}{h_1}\frac{\partial \theta}{\partial x}\right) + \cos\theta\left(K_2 + \frac{1}{h_2}\frac{\partial \theta}{\partial \phi}\right)\right]$$

$$K_{21} = \frac{1}{\sin\theta}\left[-\left(K_2 + \frac{1}{h_2}\frac{\partial \theta}{\partial \phi}\right) + \cos\theta\left(K_1 + \frac{1}{h_1}\frac{\partial \theta}{\partial x}\right)\right]$$

6.0 REFERENCES

1. Keller, H.B. and Cebeci, T.: Accurate Numerical Methods for Boundary Layers. II. Two-Dimensional Turbulent Flows. AIAA Journal, Vol. 10, Sept. 1972, pp. 1197-1200.

2. Cebeci, T.: Calculation of Three-Dimensional Boundary Layers. Pt. 1, Swept Infinite Cylinders and Small Crossflow. AIAA J., Vol. 13, 1974, p. 779.

3. Miloh, T. and Patel, V.C.: Orthogonal Coordinate Systems for Three-Dimensional Boundary Lyaers with Particular Reference to Ship Forms. Iowa Institute of Hydraulic Research, Rept. No. 138, 1972.

4. Cebeci, T., Kaups, K., and Ramsey, J.A.: A General Method for Calculating Three-Dimensional Compressible Laminar and Turbulent Boundary Layers on Arbitrary Wings. NASA CR-2777, Jan. 1977.

5. Chang, K.C. and Patel, V.C.: Calculation of Three-Dimensional Boundary Layers on Ship Forms. Iowa Institute of Hydraulic Research, Rept. No. 176, 1975.

6. Cebeci, T. and Bradshaw, P.: Momentum Transfer in Boundary Layers. Hemisphere-McGraw-Hill, Washington, 1977.

7. Hirsh, R.S. and Cebeci, T.: Calculation of Three-Dimensional Boundary Layers with Negative Crossflow on Bodies of Revolution. To be presented at AIAA 10th Fluid and Plasma Dynamics Conference, June 1977.

8. Krause, E., Hirschel, E.H., and Bothmann, Th.: Die numerische intergration der bewegungsgleichungen dreidimensionaler laminarer kompressibler grenzschichten. Fachtagung Aerodynamik, Berlin 1968, D6LR-Fachinchreike, Bond 3, 1969.

9. Cebeci, T.: On the Solution of Laminar Flow Over a Circular Cylinder Started Impulsively from Rest. In "Professor A. Walz' 70th Birthday Anniversary Volume," to be published, 1977.

10. Harder, R.L. and Besmarais, R.N.: Interpolation Using Surface Splines. J. of Aircraft, Vol. 9, No. 2, Feb. 1972, pp. 189-191.

11. James, R.M.: Practical Curve Fitting, Smoothing and Data Handling Using Fourier Analysis. Douglas Aircraft Company Report No. MDC J5832, 1975.

APPENDIX A

CALCULATION OF GEOMETRIC PARAMETERS OF THE COORDINATE SYSTEM

As discussed in Section 2.3, the geometrical parameters and external velocity components along the adopted coordinates require the quantities f_x, f_z, etc., on a ship hull. A ship hull is usually described in the form of a family of curves. For example, it may be given as the curves generated by the intersection of the hull with planes (x = constant) perpendicular to the free surface at various stations along the ship hull. The problem is then to find, with sufficient accuracy, the derivatives at an arbitrary point on the hull. When the ship hull is described analytically, then these quantities and consequently the geometric parameters of the coordinate system can be computed exactly. For arbitrary ship hulls, they must be computed numerically.

The exact solutions for the three-dimensional velocity potential is not available even on a double ship model, where the free surface is treated as a rigid plane. It is usually given experimentally or calculated numerically by the method of Hess and Smith. In this method the singularities (e.g., source, dipole, vortex, etc.) are distributed on the body surface, and the governing equation is transformed from Laplace's equation in the field into a Fredholm integral equation over the body surface. This integral equation expresses the condition of zero normal velocity on the surface. To solve the integral equation numerically the body surface is divided into a large number of small surface elements, which may be plane or curved. On each element the strength of a singularity is assumed to be either constant or variable in such a way that the overall distribution may be defined by a single unknown parameter for each element. The normal-velocity boundary condition is required to hold at one so-called control point on each element. This yields a number of linear equations equal to the number of unknown parameters defining the singularity distribution. This set of equations is solved by either direct elimination or Gauss-Seidel iteration.

The direct elimination is accomplished by the Douglas-developed SOLVIT routine, which is applicable to a large full matrix that will not fit into high-speed core storage. Recently this method has been shown to be much faster than standard IBM subroutines. Once the equations have been solved, the resulting singularity distribution is then used to calculate values of fluid velocity and pressure at the control points. As can be easily understood the

control points of the potential-flow computations will not coincide with the points where the boundary layer is to be computed. There is, therefore, a need to develop a numerical method to interpolate a function of two independent variables.

There are a number of well-known numerical techniques that can be used for interpolation and differentiation of a function of one, two, or more variables. Here we shall make use of the surface splines for interpolating and obtaining the first derivatives of a function of two variables and the Fourier series expansion for finding the second derivatives.

The surface spline is based on the small deflection equation on an infinite elastic plate that deforms in bending only. The procedure is to represent the deflection due to a point load. The deflection of the entire spline is then taken as the sum of all the point load distributions subject to the boundary condition that the surface should become flat a long distance from the applied loads. This results in a system of linear equations which is solved for the spline coefficients. The final system of equations is given below. (For details of derivation, see ref. 10.)

$$\sum_{i=1}^{N} F_i = 0 \tag{A.1}$$

$$\sum_{i=1}^{N} x_i F_i = 0 \tag{A.2}$$

$$\sum_{i=1}^{N} z_i F_i = 0 \tag{A.3}$$

$$a_0 + a_1 x_j + a_2 z_j + \sum_{i=1}^{N} F_i r_{ij}^2 \ln r_{ij}^2 = w_j, \qquad j = 1,N \tag{A.4}$$

where

$$r_{ij}^2 = (x_j - x_i)^2 + (z_j - z_i)^2 \tag{A.5}$$

If the function being interpolates has one or two planes of symmetry or antisymmetry, then use can be made of images to improve the accuracy of the fit or to reduce the number of simultaneous equations. If w is symmetrical about x_0, the system of equations becomes

$$\sum_{i=1}^{N} \bar{F}_i = 0 \tag{A.6}$$

$$\sum_{i=1}^{N} z_i \bar{F}_i = 0 \tag{A.7}$$

$$a_0 + a_2 z_j + \sum_{i=1}^{N} (r_{ij}^2 \ln r_{ij}^2 + \bar{r}_{ij}^2 \ln \bar{r}_{ij}^2)\bar{F}_i = w_j \quad j = 1,N \tag{A.8}$$

where

$$\bar{r}_{ij}^2 = (x_i + x_j - 2x_0) + (z_j - z_i)^2 \tag{A.9}$$

Similar results can be obtained for z symmetry and for both x and z symmetry. The system of equations (A.1) to (A.5) is solved using the above-described SOLVIT routine.

Equation (A.4) can be differentiated to give the first derivatives of w, or the slopes of the spline

$$\frac{\partial w_j}{\partial x} = a_1 + 2 \sum_{i=1}^{N} F_i(1 + \ln r_{ij}^2)(x_j - x_i) \tag{A.10}$$

$$\frac{\partial w_j}{\partial z} = a_2 + 2 \sum_{i=1}^{N} F_i(1 + \ln r_{ij}^2)(z_j - z_i) \tag{A.11}$$

Though (A.4) can be successively differentiated to give higher-order derivatives, for example

$$\frac{\partial^2 w_j}{\partial z^2} = 2 \sum_{i=1}^{N} F_i(1 + \ln r_{ij}^2) + 4 \sum_{i=1}^{N} F_i(z_j - z_i)^2 / r_{ij}^2 \tag{A.12}$$

they are indeterminate as $(x_j, z_j) \to (x_i, z_i)$. For removing this problem, Harder and Desmarais[10] suggested replacing the term $r^2 \ln r^2$ in (A.4) with $r^2 \ln (r^2 + \varepsilon)$. Physically we apply distributed loads instead of point loads on the plate. The new generated spline surface passes through N points and has all derivatives everywhere. The difficulty of using this alternative is to determine the distribution of ε over the spline surface and Harder and Desmarais[10] did not give the relation between ε and other known quantities explicitly.

Once the values of w have been found for some constant x_i (or z_i) using the surface spline, the derivatives can be obtained by using the cubic linear spline because w is now a function of one variable. The cubic spline, in which a piecewise, third-order polynomial is used to describe a function between two discrete points, has been widely used to interpolate and find derivatives of a function of one variable because it is easily to calculate and gives generally satisfactory results.

Once the values of w and its first derivatives $\partial w/\partial x$ and $\partial w/\partial z$ have been found for some constant x_i (or z_i) using the surface spline, the second derivatives can be obtained by the Fourier series expansion method developed by James[11] at Douglas Aircraft Company. The method has the advantage that it also smoothes the data and the results are not sensitive to irregularity of the input data.

APPENDIX B

USER'S MANUAL

The present computer program is written such that various orthogonal coordinate systems can be used. In Case I, the user provides the body geometry and the corresponding inviscid velocity components on the body surface in terms of the Cartesian coordinate system. The geometrical parameters h_1, h_2, K_1, K_2 are computed internally for the coordinate system used in this report. In Case II, the user supplies the geometrical parameters and the inviscid velocity components u_e and w_e along the coordinate lines. The input data for each case is described below.

Case I

1. Read the values of ICASE, NXT and NZT in I5 Format, three variables on one card.

   ICASE 1

   NXT Total number of x-stations for computing boundary layers, $3 \leq NXT \leq 35$

   NZT Total number of z-stations for computing boundary layers, $3 \leq NZT \leq 20$

2. Read the values of X(I), I=1,2,...,NXT in F10.0 Format, one set of eight per card.

   X(I) Values of x where the boundary layers are computed in meter or ft.

   X(I) denote the Cartesian coordinates on the body.

3. Read the values of Z(K), K=1,2,...,NZT in F10.0 Format, one set of eight per card.

   Z(K) Values of z where the boundary layers are computed in meter or ft.

   Z(K) are in the Cartesian coordinates on the body. In order to get better results, a sudden change in z interval (i.e., $\Delta z_K = z_K - z_{K-1}$) should be avoided.

4. Read the values of Y, UE, VE, and WE. The variables are punched in F10.0 format, one set of four per card in the following order:

{[Y(I,K),UE(I,K),VE(I,K),WE(I,K),K=1,NZT],I=1,NXT}

Y — y-value at (x_i, z_k) on the body surface.

UE — Inviscid velocity component along x-direction at (x_i, z_k)

VE — Inviscid velocity component along y-direction at (x_i, z_k)

WE — Inviscid velocity component along z-direction at (x_i, z_k)

Here x, y, and z are in Cartesian coordinates, Y is in meter or feet and UE, VE, and WE are in m/sec or ft/sec.

5. Read TITLE in 20A4 format. It is used for identifying the problem under study. It should not be greater than the length of 80 including blank.

6. Read the variables, NXT, NZT, NXTRAN, VISC, and UREF in one card. The first three variables are in I5 Format, the remaining variables in F10.0 Format.

NXT — Total number of x-stations for computing boundary layers, $3 \leq NXT \leq 35$

NZT — Total number of z-stations for computing boundary layers, $3 \leq NZT \leq 20$

NXTRAN — Number of x-stations at which the flow changes from laminar to turbulent. If the flow is laminar, set the value arbitrarily greater than NXT.

VISC — Kinematic viscosity of the fluid, in m^2/sec or ft^2/sec.

UREF — A reference velocity, in m/sec or ft/sec.

Case II

In Case II, the input data are almost the same as for Case I except for the following changes:

a. ICASE set equal to 2.

b. X(I) and Z(K) are given in the corresponding coordinate system instead of the Cartesian coordinate system.

c. Replace the data described in item 4 by

{[UE(I,K),WE(I,K),H1(I,K),H2(I,K),CK1(I,K),CK2(I,K),K=1,NZT], I=1,NXT}

The variables are punched in F10.0 format, six variables in one card

UE	Inviscid velocity component along x-direction
WE	Inviscid velocity component along z-direction
H1	Metric coefficient along x-direction, h_1
H2	Metric coefficient along z-direction, h_2
CK1	Geodesic curvature coefficient K_1, see (2.5)
CK2	Geodesic curvature coefficient K_2, see (2.5)

DISTRIBUTION LIST

Technical Library
Building 313
Ballistic Research Laboratories
Aberdeen Proving Ground, MD 21005

Dr. F. D. Bennett
External Ballistic Laboratory
Ballistic Research Laboratories
Aberdeen Proving Ground, MD 21005

Mr. C. C. Hudson
Sandia Corporation
Sandia Base
Albuquerque, NM 81115

Professor P. J. Roache
Ecodynamics Research
Associates, Inc.
P. O. Box 8172
Albuquerque, NM 87108

Dr. J. D. Shreve, Jr.
Sandia Corporation
Sandia Base
Albuquerque, NM 81115

Defense Documentation Center
Cameron Station, Building 5
Alexandria, VA 22314 (12)

Library
Naval Academy
Annapolis, MD 21402

Dr. G. H. Heilmeier
Director, Defense Advanced
Research Projects Agency
1400 Wilson Boulevard
Arlington, VA 22209

Mr. R. A. Moore
Deputy Director, Tactical
Technology Office
Defense Advanced Research Projects
Agency
1400 Wilson Boulevard
Arlington, VA 22209

Office of Naval Research
Code 411
Arlington, VA 22217

Office of Naval Research
Code 421
Arlington, VA 22217

Office of Naval Research
Code 438
Arlington, VA 22217

Office of Naval Research
Code 1021P (ONRL)
Arlington, VA 22217 (6)

Dr. J. L. Potter
Deputy Director, Technology
von Karman Gas Dynamics Facility
Arnold Air Force Station, TN 37389

Professor J. C. Wu
Georgia Institute of Technology
School of Aerospace Engineering
Atlanta, GA 30332

Library
Aerojet-General Corporation
6352 North Irwindale Avenue
Azusa, CA 91702

NASA Scientific and Technical
Information Facility
P. O. Box 8757
Baltimore/Washington International
Airport
Maryland 21240

Dr. S. A. Berger
University of California
Department of Mechanical Engineering
Berkeley, CA 94720

Professor A. J. Chorin
University of California
Department of Mathematics
Berkeley, CA 94720

Professor M. Holt
University of California
Department of Mechanical Engineering
Berkeley, CA 94720

Dr. L. Talbot
University of California
Department of Mechanical Engineering
Berkeley, CA 94720

Dr. H. R. Chaplin
Code 16
David W. Taylor Naval Ship Research
and Development Center
Bethesda, MD 20084

Code 1800
David W. Taylor Naval Ship Research
and Development Center
Bethesda, MD 20084

Code 5643
David W. Taylor Naval Ship Research
and Development Center
Bethesda, MD 20084

Dr. G. R. Inger
Virginia Polytechnic Institute
and State University
Department of Aerospace Engineering
Blacksburg, VA 24061

Professor A. H. Nayfeh
Virginia Polytechnic Institute
and State University
Department of Engineering Science
and Mechanics
Blacksburg, VA 24061

Indiana University
School of Applied Mathematics
Bloomington, IN 47401

Director
Office of Naval Research Branch
Office
495 Summer Street
Boston, MA 02210

Supervisor, Technical Library
Section
Thiokol Chemical Corporation
Wasatch Division
Brigham City, UT 84302

Dr. G. Hall
State University of New York at
Buffalo
Faculty of Engineering and
Applied Science
Fluid and Thermal Sciences Laboratory
Buffalo, NY 14214

Mr. R. J. Vidal
Calspan Corporation
Aerodynamics Research Department
P. O. Box 235
Buffalo, NY 14221

Professor R. F. Probstein
Massachusetts Institute of Technology
Department of Mechanical Engineering
Cambridge, MA 02139

Director
Office of Naval Research Branch Office
536 South Clark Street
Chicago, IL 60605

Code 753
Naval Weapons Center
China Lake, CA 93555

Mr. J. Marshall
Code 4063
Naval Weapons Center
China Lake, CA 93555

Professor R. T. Davis
University of Cincinnati
Department of Aerospace Engineering
and Applied Mechanics
Cincinnati, OH 45221

Library MS 60-3
NASA Lewis Research Center
21000 Brookpark Road
Cleveland, OH 44135

Dr. J. D. Anderson, Jr.
Chairman, Department of Aerospace
Engineering
College of Engineering
University of Maryland
College Park, MD 20742

Professor W. L. Melnik
University of Maryland
Department of Aerospace Engineering
Glenn L. Martin Institute of Technology
College Park, MD 20742

Professor O. Burggraf
Ohio State University
Department of Aeronautical and Astronautical Engineering
1314 Kinnear Road
Columbus, OH 43212

Technical Library
Naval Surface Weapons Center
Dahlgren Laboratory
Dahlgren, VA 22448

Dr. F. Moore
Naval Surface Weapons Center
Dahlgren Laboratory
Dahlgren, VA 22448

Technical Library 2-51131
LTV Aerospace Corporation
P. O. Box 5907
Dallas, TX 75222

Library, United Aircraft Corporation
Research Laboratories
Silver Lane
East Hartford, CT 06108

Technical Library
AVCO-Everett Research Laboratory
2385 Revere Beach Parkway
Everett, MA 02149

Professor G. Moretti
Polytechnic Institute of New York
Long Island Center
Department of Aerospace Engineering and Applied Mechanics
Route 110
Farmingdale, NY 11735

Professor S. G. Rubin
Polytechnic Institute of New York
Long Island Center
Department of Aerospace Engineering and Applied Mechanics
Route 110
Farmingdale, NY 11735

Technical Documents Center
Army Mobility Equipment R&D Center
Building 315
Fort Belvoir, VA 22060

Dr. W. R. Briley
Scientific Research Associates, Inc.
P. O. Box 498
Glastonbury, CT 06033

Library (MS 185)
NASA Langley Research Center
Langley Station
Hampton, VA 23665

Dr. S. Nadir
Northrop Corporation
Aircraft Division
3901 West Broadway
Hawthorne, CA 90250

Professor A. Chapmann
Chairman, Mechanical Engineering Department
William M. Rice Institute
Box 1892
Houston, TX 77001

Dr. F. Lane
KLD Associates, Inc.
7 High Street
Huntington, NY 11743

Technical Library
Naval Ordnance Station
Indian Head, MD 20640

Professor D. A. Caughey
Cornell University
Sibley School of Mechanical and Aerospace Engineering
Ithaca, NY 14853

Professor E. L. Resler
Cornell University
Sibley School of Mechanical and Aerospace Engineering
Ithaca, NY 14853

Professor S. F. Shen
Cornell University
Sibley School of Mechanical and Aerospace Engineering
Ithaca, NY 14853

Library
Midwest Research Institute
425 Volker Boulevard
Kansas City, MO 64110

Dr. M. M. Hafez
Flow Research, Inc.
P. O. Box 5040
Kent, WA 98031

Dr. E. M. Murman
Flow Research, Inc.
P. O. Box 5040
Kent, WA 98031

Dr. S. A. Orszag
Cambridge Hydrodynamics, Inc.
54 Baskin Road
Lexington, MA 02173

Professor T. Cebeci
California State University, Long Beach
Mechanical Engineering Department
Long Beach, CA 90840

Mr. J. L. Hess
Douglas Aircraft Company
3855 Lakewood Boulevard
Long Beach, CA 90808

Dr. H. K. Cheng
University of Southern California, University Park
Department of Aerospace Engineering
Los Angeles, CA 90007

Professor J. D. Cole
University of California
Mechanics and Structures Department
School of Engineering and Applied Science
Los Angeles, CA 90024

Engineering Library
University of Southern California
Box 77929
Los Angeles, CA 90007

Dr. C. -M. Ho
University of Southern California, University Park
Department of Aerospace Engineering
Los Angeles, CA 90007

Dr. T. D. Taylor
The Aerospace Corporation
P. O. Box 92957
Los Angeles, CA 90009

Commanding Officer
Naval Ordnance Station
Louisville, KY 40214

Mr. B. H. Little, Jr.
Lockheed-Georgia Company
Department 72-74, Zone 369
Marietta, GA 30061

Dr. C. Cook
Stanford Research Institute
Menlo Park, CA 94025

Professor E. R. G. Eckert
University of Minnesota
241 Mechanical Engineering Building
Minneapolis, MN 55455

Library
Naval Postgraduate School
Monterey, CA 93940

McGill University
Supersonic-Gas Dynamics Research Laboratory
Department of Mechanical Engineering
Montreal 12, Quebec, Canada

Librarian
Engineering Library, 127-223
Radio Corporation of America
Morristown, NJ 07960

Dr. S. S. Stahara
Nielsen Engineering & Research, Inc.
510 Clyde Avenue
Mountain View, CA 94043

Engineering Societies Library
345 East 47th Street
New York, NY 10017

Professor A. Jameson
New York University
Courant Institute of Mathematical Sciences
251 Mercer Street
New York, NY 10012

Professor G. Miller
New York University
Department of Applied Science
26-36 Stuyvesant Street
New York, NY 10003

Office of Naval Research
New York Area Office
715 Broadway - 5th Floor
New York, NY 10003

Dr. A. Vaglio-Laurin
New York University
Department of Applied Science
26-36 Stuyvesant Street
New York, NY 10003

Professor S. Weinbaum
Research Foundation of the City
University of New York on behalf
of the City College
1411 Broadway
New York, NY 10018

Librarian, Aeronautical Library
National Research Council
Montreal Road
Ottawa 7, Canada

Lockheed Missiles and Space Company
Technical Information Center
3251 Hanover Street
Palo Alto, CA 94304

Director
Office of Naval Research Branch
Office
1030 East Green Street
Pasadena, CA 91106

California Institute of Technology
Engineering Division
Pasadena, CA 91109

Library
Jet Propulsion Laboratory
4800 Oak Grove Drive
Pasadena, CA 91103

Professor H. Liepmann
California Institute of Technology
Department of Aeronautics
Pasadena, CA 91109

Mr. L. I. Chasen, MGR-MSD Lib.
General Electric Company
Missile and Space Division
P. O. Box 8555
Philadelphia, PA 19101

Mr. P. Dodge
Airesearch Manufacturing Company
of Arizona
Division of Garrett Corporation
402 South 36th Street
Phoenix, AZ 85034

Technical Library
Naval Missile Center
Point Mugu, CA 93042

Professor S. Bogdonoff
Princeton University
Gas Dynamics Laboratory
Department of Aerospace and
Mechanical Sciences
Princeton, NJ 08540

Professor S. I. Cheng
Princeton University
Department of Aerospace and
Mechanical Sciences
Princeton, NJ 08540

Dr. J. E. Yates
Aeronautical Research Associates
of Princeton, Inc.
50 Washington Road
Princeton, NJ 08540

Professor J. H. Clarke
Brown University
Division of Engineering
Providence, RI 02912

Professor J. T. C. Liu
Brown University
Division of Engineering
Providence, RI 02912

Professor L. Sirovich
Brown University
Division of Applied Mathematics
Providence, RI 02912

Dr. P. K. Dai (R1/2178)
TRW Systems Group, Inc.
One Space Park
Redondo Beach, CA 90278

Redstone Scientific Information Center
Chief, Document Section
Army Missile Command
Redstone Arsenal, AL 35809

U.S. Army Research Office
P. O. Box 12211
Research Triangle, NC 27709

Professor M. Lessen
The University of Rochester
Department of Mechanical Engineering
River Campus Station
Rochester, NY 14627

Editor, Applied Mechanics Review
Southwest Research Institute
8500 Culebra Road
San Antonio, TX 78228

Library and Information Services
General Dynamics-CONVAIR
P. O. Box 1128
San Diego, CA 92112

Dr. R. Magnus
General Dynamics-CONVAIR
Kearny Mesa Plant
P. O. Box 80847
San Diego, CA 92138

Mr. T. Brundage
Defense Advanced Research Projects Agency
Research and Development Field Unit
APO 146, Box 271
San Francisco, CA 96246

Office of Naval Research
San Francisco Area Office
760 Market Street - Room 447
San Francisco, CA 94102

Library
The Rand Corporation
1700 Main Street
Santa Monica, CA 90401

Department Librarian
University of Washington
Department of Aeronautics and Astronautics
Seattle, WA 98105

Dr. P. E. Rubbert
Boeing Commercial Airplane Company
P. O. Box 3707
Seattle, WA 98124

Mr. R. Feldhuhn
Naval Surface Weapons Center
White Oak Laboratory
Silver Spring, MD 20910

Dr. G. Heiche
Naval Surface Weapons Center
Mathematical Analysis Branch
Silver Spring, MD 20910

Librarian
Naval Surface Weapons Center
White Oak Laboratory
Silver Spring, MD 20910

Dr. J. M. Solomon
Naval Surface Weapons Center
White Oak Laboratory
Silver Spring, MD 20910

Professor J. H. Ferziger
Stanford University
Department of Mechanical Engineering
Stanford, CA 94305

Professor K. Karamcheti
Stanford University
Department of Aeronautics and Astronautics
Stanford, CA 94305

Professor M. van Dyke
Stanford University
Department of Aeronautics and Astronautics
Stanford, CA 94305

Engineering Library
McDonnell Douglas Corporation
Department 218, Building 101
P. O. Box 516
St. Louis, MO 63166

Dr. R. J. Hakkinen
McDonnell Douglas Corporation
Department 222
P. O. Box 516
St. Louis, MO 63166

Dr. R. P. Heinisch
Honeywell, Inc.
Systems and Research Division -
Aerospace Defense Group
2345 Walnut Street
St. Paul, MN 55113

Professor R. G. Stoner
Arizona State University
Department of Physics
Tempe, AZ 85721

Dr. N. Malmuth
Rockwell International
Science Center
1049 Camino Dos Rios
P. O. Box 1085
Thousand Oaks, CA 91360

Rockwell International
Science Center
1049 Camino Dos Rios
P. O. Box 1085
Thousand Oaks, CA 91360

The Library
University of Toronto
Institute of Aerospace Studies
Toronto 5, Canada

Professor W. R. Sears
University of Arizona
Aerospace and Mechanical Engineering
Tucson, AZ 85721

Professor A. R. Seebass
University of Arizona
Department of Aerospace and
Mechanical Engineering
Tucson, AZ 85721

Dr. S. M. Yen
University of Illinois
Coordinated Science Laboratory
Urbana, IL 61801

Dr. K. T. Yen
Code 3015
Naval Air Development Center
Warminster, PA 18974

Air Force Office of Scientific
Research (SREM)
Building 1410, Bolling AFB
Washington, DC 20332

Chief of Research & Development
Office of Chief of Staff
Department of the Army
Washington, DC 20310

Library of Congress
Science and Technology Division
Washington, DC 20540

Director of Research (Code RR)
National Aeronautics and
Space Administration
600 Independence Avenue, SW
Washington, DC 20546

Library
National Bureau of Standards
Washington, DC 20234

National Science Foundation
Engineering Division
1800 G Street, NW
Washington, DC 20550

Mr. W. Koven (AIR 03E)
Naval Air Systems Command
Washington, DC 20361

Mr. R. Siewert (AIR 320D)
Naval Air Systems Command
Washington, DC 20361

Technical Library Division (AIR 604)
Naval Air Systems Command
Washington, DC 20361

Code 2627
Naval Research Laboratory
Washington, DC 20375

SEA 03512
Naval Sea Systems Command
Washington, DC 20362

SEA 09G3
Naval Sea Systems Command
Washington, DC 20362

Dr. A. L. Slafkosky
Scientific Advisor
Commandant of the Marine Corps
(Code AX)
Washington, DC 20380

Director
Weapons Systems Evaluation Group
Washington, DC 20305

Dr. P. Baronti
General Applied Science
Laboratories, Inc.
Merrick and Stewart Avenues
Westbury, NY 11590

Bell Laboratories
Whippany Road
Whippany, NJ 07981

Chief of Aerodynamics
AVCO Corporation
Missile Systems Division
201 Lowell Street
Wilmington, MA 01887

Research Library
AVCO Corporation
Missile Systems Division
201 Lowell Street
Wilmington, MA 01887

AFAPL (APRC)
AB
Wright Patterson, AFB, OH 45433

Dr. Donald J. Harney
AFFDL/FX
Wright Patterson AFB, OH 45433